

Absorption spectrum of clusters of spheres from the general solution of Maxwell's equations. II. Optical properties of aggregated metal spheres

J. M. Gérardy and M. Ausloos

Université de Liège, Institut de Physique, B5, 4000 Sart Tilman-Liège 1, Belgium

(Received 26 February 1981)

A very general theory for the infrared absorption spectrum of homogeneous sphere clusters is presented. Maxwell's equations are solved for any arbitrary cluster geometry and for any light (polarized or not) incidence by usual expansions of the various fields. Usual boundary conditions are used but take into account the possible existence of plasmons in the spheres. High-order multipolar (electric and magnetic) interaction effects are included. The problem is cast into the calculation of the microscopic effective dielectric and magnetic susceptibility for the spheres, and that of the appropriate interaction terms. The latter (which constitute the hardest part of the theory in general) are calculated by formulating in a very practical way a recurrence relation for spherical vector wave functions in different reference frames. The extinction cross section is derived for any arbitrary case in order to allow for comparison of experimental data and previous theoretical work. The theory in the absence of any high-order polar effect is applied to the case of metallic clusters, e.g., small sodium spheres. Effects due to size distribution, sphere separation, and sphere magnetic permittivity are analyzed. Different light incidences are considered. A very brief discussion of the experimental status is presented for the case of metallic spheres. New experiments are suggested for which the theory is easily read out. Appendices contain new relations between Legendre functions and "spherical coupling parameters" allowing one to treat up to $(2^4, 2^4)$ polar-order interactions.

I. INTRODUCTION

We have recently presented a theory of the infrared absorption spectrum of ionic powders (modeled by clusters of spherules) by solving Laplace's equation up to a given 2^s polar order in the long-wavelength limit.¹ Numerical results have been presented at topical conferences. Effects due to quadrupolar and octupolar field fluctuations in the particles were shown to be very important.²⁻⁴ The neglect of retardation effect has been briefly discussed.¹ Owing to recent experimental advances,^{5,6} it appears of interest to extend our work to the case of metallic aggregates and more complex systems, like those including oxide layers or dielectric nuclei. The latter situation will be described in Paper III of this series. Here we present a general theory for the case of clusters of homogeneous metallic spheres. Since we have demonstrated the effect of dipole-dipole indirect exchange through high polar order in ionic systems,²⁻⁴ it seems important to include such couplings between metallic particles from the beginning.

Our theory will be general enough to include even magnetic multipolar orders and the coupling of them to the electric multipoles. Nevertheless, at the numerical stage a finite number of multipoles only will be taken into account.

The spherical shape restriction could be phenomenologically removed by introducing depolarization factors to take into account the oblateness of particles. Similarly the homogeneity condition may not be very drastic and can be easily removed. Such extensions may be done following work by various authors⁷⁻⁹ extending the Clippe-Evrard-Lucas (CEL) theory.^{10,11} Nevertheless, let us recall that the latter is restricted to dipole fluctuations and direct dipole-dipole coupling only.

Either following CEL theory or under various approximations (noninteracting particles, e.g.), much work has already been presented on optical properties of small metallic spheres. Following the Mie theory,¹² Wyath presented some extension to take into account inhomogeneities.¹³ Clanget,¹⁴ Simanek,⁸ and Ruppin¹⁵ have studied independent particles. We will closely follow Ruppin's method, but add an important ingredient as demonstrated

for ionic powders: the clustering effects.^{3,11}

In Sec. II the generalization of the classical Mie theory as modified by Ruppin to take into account plasmon distribution in isolated metallic spheres, is presented. In the absence of plasmons the theory is an extension of that presented in Ref. 1, since we take into account here magnetic permeability and retardation effects.

The general theory is presented as follows: the single-sphere case (for introducing notations and recalling properties of spherical wave functions) is followed by the N -particle case. The formal solution of Maxwell's equation is established, accounting for usual boundary conditions. The interaction terms are then calculated by formulating in a very practical way a recurrence relation for functions described in different reference frames. We then derive the general formula for the extinction cross section, allowing us some comparison to experimental data and previous theoretical work.

The theory is so far valid for ionic or metallic constituents since the dielectric and magnetic constants are not specified. In Sec. III we treat as examples the modification in the extinction cross section of a pair of sodium spheres with respect to that of isolated spheres (Ruppin theory¹⁵), as well as that of an infinite linear chain of identical sodium spheres. Different light incidences are considered.

In Sec. IV our discussion concerns the possibility of experimental observation and hence takes into account the influence of different parameters: radii distributions and sphere-separation effects. Multipolar effects are not discussed here. Appendix A contains relations between Legendre functions as

$$[q(q+1)]^{1/2} \vec{m}_{qp} = ipz_q(kr) \frac{Y_{qp}(\theta, \varphi)}{\sin\theta} \vec{1}_\theta - z_q(kr) \frac{\partial Y_{qp}(\theta, \varphi)}{\partial\theta} \vec{1}_\varphi, \quad (2a)$$

$$[q(q+1)]^{1/2} \vec{n}_{qp} = q(q+1) \frac{z_q(kr)}{kr} Y_{qp}(\theta, \varphi) \vec{1}_r + \frac{[krz_q(kr)]'}{kr} \frac{\partial Y_{qp}(\theta, \varphi)}{\partial\theta} \vec{1}_\theta + ip \frac{[krz_q(kr)]'}{kr} \frac{Y_{qp}(\theta, \varphi)}{\sin\theta} \vec{1}_\varphi, \quad (2b)$$

$$[q(q+1)]^{1/2} \vec{1}_{qp} = k \left[z_q'(kr) Y_{qp}(\theta, \varphi) \vec{1}_r + \frac{z_q(kr)}{kr} \frac{\partial Y_{qp}(\theta, \varphi)}{\partial\theta} \vec{1}_\theta + ip \frac{z_q(kr)}{kr} \frac{Y_{qp}(\theta, \varphi)}{\sin\theta} \vec{1}_\varphi \right], \quad (2c)$$

where the prime stands for a derivative with respect to the argument. The principal properties of these functions have to be recalled¹⁶:

$$\vec{m}_{qp} = \vec{\nabla} \times (\vec{r} \xi_{qp}) = \vec{1}_{qp} \times \vec{r} = \frac{1}{k} \vec{\nabla} \times \vec{n}_{qp} \quad (3a)$$

used for the transposition of frames. In Appendix B, explicit values of the solution of the recurrence equation for the projected potential functions are given, allowing any consideration of up to the 2⁴th polar interaction order.

II. EXTENDED MIE-RUPPIN THEORY FOR METALLIC CLUSTERS

A. Single-sphere case

Consider a spherical particle embedded in an infinite matrix and submitted to an electromagnetic field. The Maxwell equations are

$$\vec{\nabla} \times \vec{H} = \frac{1}{c} \frac{\partial \vec{E}}{\partial t} + \frac{4\pi}{c} \vec{J}, \quad (1a)$$

$$\vec{\nabla} \times \vec{E} = -\frac{1}{c} \frac{\partial \vec{B}}{\partial t}, \quad (1b)$$

$$\vec{\nabla} \cdot \vec{B} = 0, \quad (1c)$$

where \vec{H} is the magnetic field, \vec{E} is the electric field, \vec{J} is the sum of the polarization and diffusion currents, and \vec{B} is the magnetic induction. We suppose that the time dependence of all these quantities is proportional to $e^{-i\omega t}$. The fields are not supposed to be too high such that the current \vec{J} can be taken as proportional to the field \vec{E} . It is useful to derive the solutions of Eq. (1) in terms of spherical harmonics. Let us introduce the three independent spherical wave-vector functions^{16,17} \vec{m}_{qp} , \vec{n}_{qp} , and $\vec{1}_{qp}$ (the definition in Ref. 16 is in terms of Legendre polynomials):

$$\vec{n}_{qp} = \vec{\nabla} \times \vec{\nabla} \times (\vec{r} \xi_{qp}) = \frac{1}{k} \vec{\nabla} \times \vec{m}_{qp} \quad (3b)$$

for the functions corresponding to a transverse wave, while

$$\vec{1}_{qp} = \vec{\nabla} \xi_{qp} \quad (3c)$$

for the longitudinal wave, where the "potential" ξ_{qp} is

$$\xi_{qp} = z_q(kr)Y_{qp}(\theta, \varphi)[q(q+1)]^{-1/2}. \quad (4)$$

Furthermore

$$\vec{\nabla} \cdot \vec{m}_{qp} = \vec{\nabla} \cdot \vec{n}_{qp} = 0 \quad (5a)$$

$$\vec{\nabla} \cdot \vec{l}_{qp} \neq 0 \quad (5b)$$

$$\vec{\nabla} \times \vec{l}_{qp} = 0. \quad (5c)$$

In Eqs. (2) and (3), the z_q are the Bessel spherical functions¹⁸ $j_q, y_q, h_q^{(1)},$ or $h_q^{(2)}$. Which Bessel function has to be chosen depends on the required asymptotic behavior at zero or at infinity. The $Y_{qp}(\theta, \varphi)$'s are the usual normalized spherical harmonics. The functions are hereby defined at a point $\vec{r}(r, \theta, \varphi)$ for which the spherical-frame basis $(\vec{l}_r, \vec{l}_\theta, \vec{l}_\varphi)$ is easily related to a Cartesian frame $(\vec{l}_x, \vec{l}_y, \vec{l}_z)$.

The complex wave number k is given by the dispersion relation

$$k^2 = \frac{\omega^2}{c^2} \epsilon^T(k, \omega) \mu(k, \omega) \quad (6a)$$

for transversal waves, where ω is the frequency, c is the light velocity, $\epsilon^T(k, \omega)$ is the transverse dielectric constant, and $\mu(k, \omega)$ the magnetic permeability of the appropriate medium. For longitudinal waves we have

$$\epsilon^L(k, \omega) = 0, \quad (6b)$$

where $\epsilon^L(k, \omega)$ is the longitudinal dielectric constant. Solutions of Eqs. (6) are chosen such that k has a positive imaginary part. Furthermore, we consider that there is no longitudinal plasmon in the matrix (this supposition leads to a divergenceless electric field).

Then the electromagnetic wave (\vec{E}_M, \vec{H}_M) in the matrix can be expanded as

$$\vec{E}_M = E_0 \sum_{q,p} (\alpha_{qp}^M \vec{m}_{qp1} + \mathcal{L}_{qp}^M \vec{n}_{qp1} + c_{qp}^M \vec{m}_{qp3} + \mathcal{L}'_{qp}^M \vec{n}_{qp3}) \quad (7a)$$

$$\vec{H}_M = H_0 \sum_{q,p} (\mathcal{L}_{qp}^M \vec{m}_{qp1} + \alpha_{qp}^M \vec{n}_{qp1} + \mathcal{L}'_{qp}^M \vec{m}_{qp3} + c_{qp}^M \vec{n}_{qp3}). \quad (7b)$$

The summation is taken for $q = 1$ up to infinity and $p = -q$ up to $+q$. The subscript 1 or 3 indi-

cates which Bessel functions to use; j_q or $h_q^{(1)}$. The \vec{l}_{qp} functions do not appear here because they describe longitudinal fields [see Eqs. (5b) and (5c)]. Using Eqs. (1b), (3a), and (3b), we have

$$H_0 = \frac{ck}{i\omega\mu} E_0, \quad (8)$$

where $k(\mu)$ is the wave number (the magnetic permeability) of the matrix. The coefficients α_{qp}^M and \mathcal{L}_{qp}^M describe the incident waves (which are not yet fixed), and the coefficients c_{qp}^M and \mathcal{L}'_{qp}^M describe the waves diffracted by the sphere. E_0 is the amplitude of the electric field experimentally created.

We assume the existence of longitudinal plasmons inside the uniform sphere. Then the fields can be expanded as follows:

$$\vec{E} = E_0 \sum_{q,p} (\alpha_{qp} \vec{m}_{qp1} + \mathcal{L}_{qp} \vec{n}_{qp1} + e_{qp} \vec{l}_{qp1}) \quad (9a)$$

$$\vec{H} = H_j \sum_{q,p} (\mathcal{L}'_{qp} \vec{m}_{qp1} + \alpha_{qp} \vec{n}_{qp1}). \quad (9b)$$

Notice that the longitudinal plasmons do not directly influence the magnetic field [see Eq. (5c)]. The following relation

$$H_j = \frac{ck_j^T}{i\omega\mu_j} E_0 \quad (10)$$

holds between the amplitudes H_j and E_0 , where $k_j^T(\mu_j)$ is the transverse wave number (the magnetic permeability) inside the sphere. The "classical" boundary conditions are

$$\vec{E} \times \vec{l}_r = \vec{E}_M \times \vec{l}_r \quad (11a)$$

$$\vec{H} \times \vec{l}_r = \vec{H}_M \times \vec{l}_r. \quad (11b)$$

Because of the existence of longitudinal waves, we must add to this system a third condition discussed by Melnyk and Harrison.¹⁹

$$\vec{E} \cdot \vec{l}_r = \vec{E}_M \cdot \vec{l}_r. \quad (11c)$$

The calculation is then the same as that developed by Ruppin¹⁵ in the case $\mu_j = \mu = 1$, and leads to the following relations:

$$\mathcal{L}_{qp}^M = \Delta_q \mathcal{L}_{qp}^M, \quad (12a)$$

$$c_{qp}^M = \Gamma_q \alpha_{qp}^M, \quad (12b)$$

where Δ_q and Γ_q are the 2^q polar electrical and magnetic susceptibilities of the sphere. They are explicitly given by

$$\Delta_q = - \left[\frac{j_q(kR)}{h_q^{(1)}(kR)} \right] \left[\frac{\epsilon[j_q^\dagger(k_j^T R) - f_q(k_j^L R)] - \epsilon_j^T[j_q^\dagger(kR) - f_q(k_j^L R)]}{\epsilon[j_q^\dagger(k_j^T R) - f_q(k_j^L R)] - \epsilon_j^T[h_q^{(1)\dagger}(kR) - f_q(k_j^L R)]} \right] \quad (12c)$$

$$\Gamma_q = - \left[\frac{j_q(kR)}{h_q^{(1)}(kR)} \right] \left[\frac{\mu_j j_q^\dagger(k_j^T R) - \mu_j j_q^\dagger(kR)}{\mu_j j_q^\dagger(k_j^T R) - \mu_j h_q^{(1)\dagger}(kR)} \right]. \quad (12d)$$

In the above equations, a given function $g^\dagger(z)$ is defined by

$$g^\dagger(z) = \frac{1}{g(z)} \frac{d}{dz} [zg(z)], \quad (13)$$

while the function $f_q(z)$ is defined by

$$f_q(z) = q(q+1)j_q(z) \left/ \left[z \frac{d}{dz} j_q(z) \right] \right., \quad (14)$$

where R is the radius of the sphere, k_j^L , ϵ_j^L are, respectively, the longitudinal wave number and dielectric constant inside the sphere, and ϵ_j^T is the transverse dielectric constant inside the sphere.

When there is no longitudinal plasmon inside the sphere, the imaginary part of k_j^L tends to infinity and $f_q(k_j^L R)$ vanishes. In this case, the electrical susceptibilities Δ_q are similar to the magnetic susceptibilities Γ_q with the interchange $\epsilon \leftrightarrow \mu$. Notice the important result that the magnetic susceptibilities are not influenced by the longitudinal plasmons. An interesting extension not considered here would be to include (anisotropic) dispersion relations for magnons in order to couple these excitations to the oscillating magnetic field. Optical properties of magnetic (metallic or ionic) particles present, nevertheless, some well known interest.²⁰⁻²³

B. N -spheres case

As in Ref. 1, all functions and coefficients will be characterized by the index j of the sphere. In the matrix (M), the solution of the Maxwell equations is taken as the sum of the diffracted fields and the incident wave (\vec{E}_0, \vec{H}_0). Then we have

$$\vec{E}_M = E_0 \sum_{i=1}^N \sum_{q,p} [c_{qp}^M(i) \vec{m}_{qp3}(i) + \mathcal{L}_{qp}^M(i) \vec{n}_{qp3}(i)] + \vec{E}_0 \quad (15a)$$

$$\vec{H}_M = H_0 \sum_{i=1}^N \sum_{q,p} [\mathcal{A}_{qp}^M(i) \vec{m}_{qp3}(i) + c_{qp}^M(i) \vec{n}_{qp3}(i)] + \vec{H}_0. \quad (15b)$$

The functions $\vec{m}_{qp}(i)$ and $\vec{n}_{qp}(i)$ are defined in the i frame centered on the i sphere. Consider now the j

sphere. Stratton¹⁶ has shown that the system formed by \vec{m}_{qp} and \vec{n}_{qp} is orthogonal and complete for transverse waves. Thus, by using a projection technique one has

$$\vec{m}_{qp3}(i) = \sum_{l,m} [\langle \vec{m}_{qp3}(i) | \vec{m}_{lm1}(j) \rangle \vec{m}_{lm1}(j) + \langle \vec{m}_{qp3}(i) | \vec{n}_{lm1}(j) \rangle \vec{n}_{lm1}(j)], \quad (16a)$$

$$\vec{n}_{qp3}(i) = \sum_{l,m} [\langle \vec{n}_{qp3}(i) | \vec{m}_{lm1}(j) \rangle \vec{m}_{lm1}(j) + \langle \vec{n}_{qp3}(i) | \vec{n}_{lm1}(j) \rangle \vec{n}_{lm1}(j)], \quad (16b)$$

where

$$\langle \vec{m}_{qp3}(i) | \vec{m}_{lm1}(j) \rangle = \frac{\int \int \vec{m}_{qp3}(i) \cdot \vec{m}_{lm1}^*(j) d\Omega_j}{\int \int |\vec{m}_{lm1}(j)|^2 d\Omega_j}, \quad (17)$$

with similar definitions for the other terms. The integrals are taken on the polar angles θ_j and φ_j defined in the j frame ($d\Omega_j = \sin\theta_j d\theta_j d\varphi_j$). It can be proven that those terms do not depend on the \vec{r} position in space, and depend only on the vector \vec{a}_{ji} joining the center of the particle j to the center of the particle i . Expansions (16) are only valid for a point \vec{r} inside a sphere centered on the origin of the frame j with a radius $R = |\vec{a}_{ji}|$. From Eq. (3) it follows that

$$\langle \vec{m}_{qp3}(i) | \vec{m}_{lm1}(j) \rangle = \langle \vec{n}_{qp3}(i) | \vec{n}_{lm1}(j) \rangle \equiv \mathcal{T}_{qplm}(i,j) \quad (18a)$$

$$\langle \vec{m}_{qp3}(i) | \vec{n}_{lm1}(j) \rangle = \langle \vec{n}_{qp3}(i) | \vec{m}_{lm1}(j) \rangle \equiv \mathcal{C}_{qplm}(i,j). \quad (18b)$$

The choice of the Bessel functions j_j in the projection functions $\vec{m}_{lm1}(j)$ and $\vec{n}_{lm1}(j)$ is determined by their behavior at $\vec{r}=0$. Using Eq. (16), it is then easy to relate the fields \vec{E}_M and \vec{H}_M in a frame centered on a j sphere to that in an i frame.

In order to complete the expansion, we write the incident wave in the vicinity of the j sphere as follows:

$$\vec{E}_0 = E_0 \sum_{q,p} [\alpha_{qp}^I(j) \vec{m}_{qp1}(j) + \mathcal{L}_{qp}^I(j) \vec{n}_{qp1}(j)] \quad (19a)$$

$$\vec{H}_0 = H_0 \sum_{q,p} [\mathcal{L}_{qp}^I(j) \vec{m}_{qp1}(j) + \alpha_{qp}^I(j) \vec{n}_{qp1}(j)]. \quad (19b)$$

If we compare Eqs. (15) and (7) with the additional subscript j , using Eqs. (16a) and (16b), the properties (18), and the expansions (19) of the incident fields, we may finally write

$$\alpha_{lm}^M(j) = \alpha_{lm}^I(j) + \sum_{q,p} \sum_{i \neq j}^N [c_{qp}^M(i) \mathcal{T}_{qplm}(i,j) + \mathcal{A}_{qp}^M(i) \mathcal{C}_{qplm}(i,j)] \quad (20a)$$

$$\mathcal{L}_{lm}^M(j) = \mathcal{L}_{lm}^I(j) + \sum_{q,p} \sum_{i \neq j}^N [c_{qp}^M(i) \mathcal{C}_{qplm}(i,j) + \mathcal{A}_{qp}^M(i) \mathcal{T}_{qplm}(i,j)]. \quad (20b)$$

Explicitly writing the relations (12) for each j particle, one obtains a set of linear equations between the unknown coefficients:

$$\begin{aligned} c_{lm}^M(j) - \Gamma_l(j) \sum_{q,p} \sum_{i \neq j}^N [c_{qp}^M(i) \mathcal{T}_{qplm}(i,j) + \mathcal{A}_{qp}^M(i) \mathcal{C}_{qplm}(i,j)] \\ = \Gamma_l(j) \alpha_{lm}^I(j) \end{aligned} \quad (21a)$$

$$\begin{aligned} \mathcal{A}_{lm}^M(j) - \Delta_l(j) \sum_{q,p} \sum_{i \neq j}^N [c_{qp}^M(i) \mathcal{C}_{qplm}(i,j) + \mathcal{A}_{qp}^M(i) \mathcal{T}_{qplm}(i,j)] \\ = \Delta_l(j) \mathcal{L}_{lm}^I(j). \end{aligned} \quad (21b)$$

In those equations, the summations over $q = [1, \infty]$ and over $p = [-q, +q]$ may be truncated in order to obtain some approximation to the fields. The above system is similar to that found in Ref. 1, but it includes here electromagnetic interactions $\mathcal{C}_{qplm}(i,j)$ as well. If these coupling terms did not exist, one would obtain two distinct sets of equations describing the electrical modes, and independently the magnetic modes. Notice that the dimension of the matrix is twice the dimension of that used in Ref. 1.

Owing to relations (18), it is possible to reformulate the solution of the system (21) into the inversion of two matrices with a dimension reduced by a factor two. Let $\underline{\Delta}^{-1}$ and $\underline{\Gamma}^{-1}$ be the diagonal matrices formed by the inverse of the susceptibilities, while $\underline{\mathcal{T}}$ and $\underline{\mathcal{C}}$ are formed from the $\mathcal{T}_{qplm}(i,j)$ and $\mathcal{C}_{qplm}(i,j)$. The $c_{lm}^M(j)$, $\mathcal{A}_{lm}^M(j)$,

$\alpha_{lm}^I(j)$, and $\mathcal{L}_{lm}^I(j)$ are defined as elements of the vectors \vec{c} , $\vec{\mathcal{A}}$, $\vec{\alpha}$, and $\vec{\mathcal{L}}$ respectively. Then the system (21) may be concisely written as

$$(\underline{\Gamma}^{-1} - \underline{\mathcal{T}}) \cdot \vec{c} - \underline{\mathcal{C}} \cdot \vec{\mathcal{A}} = \vec{\alpha} \quad (22a)$$

$$(\underline{\Delta}^{-1} - \underline{\mathcal{T}}) \cdot \vec{\mathcal{A}} - \underline{\mathcal{C}} \cdot \vec{c} = \vec{\mathcal{L}}. \quad (22b)$$

It is easy to show that the solution ($\vec{\mathcal{A}}$ and \vec{c}) of these equations is

$$\begin{aligned} \vec{c} = [(\underline{\Gamma}^{-1} - \underline{\mathcal{T}}) - \underline{\mathcal{C}} : (\underline{\Delta}^{-1} - \underline{\mathcal{T}})^{-1} : \underline{\mathcal{C}}]^{-1} \\ \times [\vec{\alpha} - \underline{\mathcal{C}} : (\underline{\Delta}^{-1} - \underline{\mathcal{T}})^{-1} : \vec{\mathcal{L}}], \end{aligned} \quad (23)$$

$$\vec{\mathcal{A}} = (\underline{\Delta}^{-1} - \underline{\mathcal{T}})^{-1} : (\vec{\mathcal{L}} - \underline{\mathcal{C}} \cdot \vec{c}), \quad (24)$$

where the matrices to be inverted have indeed a reduced dimension. Limiting the sum in Eqs. (21) to the term $q = s$, the solution of the problem implies only a calculation of the inverse of two matrices of dimension $Ns(s+2)$ and a few matrix products. The computer time can be much smaller than that necessary for the inversion of the complete matrix of dimension $2Ns(s+2)$ in Eqs. (21).

This formal solution, although rigorous, can be completed by a direct numerical calculation. It is, however, possible to obtain analytical expressions of the interacting terms (17) for any aggregate. This is made in the following subsection, and allows for a more suitable approach to numerical work.

C. Calculation of the interaction term

Langbein²⁴ has calculated interaction terms for spheres on a lattice including all high-order polar contributions. His calculation is based on a ‘‘differential-recurrence’’ equation [Eq. (5.68) in Ref. 24], which is rather impractical. He has given the solution of such a differential-recurrence relation, which leads to tedious numerical work. From such a solution, one can obtain the interaction terms previously defined.

We have been able to obtain the same solution by a more elegant method, using a purely recurrent relation between the interaction terms. The proof is rather simple and, although requiring some algebra, the method seems of general interest and of practical importance for similar problems in other fields of physics. It is a straightforward technique which may nevertheless be skipped by the reader interested only in the final result [Eq. (50) below]. In the following calculation, we simplify the writing by letting the wave number k ,

which is only a scaling factor for the distance, to be equal to unity. Consider the function $\psi_{q,p}$ defined by

$$\psi_{q,p} = z_q(r) P_q^p(\cos\theta) e^{ip\varphi}, \quad (25)$$

where the $P_q^p(\cos\theta)$'s are the Legendre functions. The function $\psi_{q,p}$ differs from ξ_{qp} given in Eq. (4) only by a scaling factor. The above new choice is made because of the simplicity in the following treatment. Consider now both operators

$$\partial_+ = \frac{\partial}{\partial x} + i \frac{\partial}{\partial y} \quad (26)$$

$$\partial_0 = \frac{\partial}{\partial z}. \quad (27)$$

We have at a point $\vec{r}(r, \theta, \varphi)$:

$$\partial_+ r = \sin\theta e^{i\varphi}, \quad (28a)$$

$$\partial_+ \cos\theta = -\cos\theta \sin\theta e^{i\varphi} / r, \quad (28b)$$

$$\partial_+ \varphi = -ie^{i\varphi} / (r \sin\theta), \quad (28c)$$

and then

$$\begin{aligned} \partial_+ \psi_{q,p} &= \frac{dz_q(r)}{dr} \sin\theta P_q^p(\cos\theta) e^{i(p+1)\varphi} \\ &\quad - \frac{z_q(r)}{r} \frac{dP_q^p(\cos\theta)}{d\cos\theta} \cos\theta \sin\theta e^{i(p+1)\varphi} \\ &\quad - p \frac{z_q(r)}{r} \frac{P_q^p(\cos\theta)}{\sin\theta} e^{i(p+1)\varphi}. \end{aligned} \quad (29)$$

The recurrence relations for spherical Bessel functions given by Eqs. (10.1.19) and (10.1.20) in Ref. 18, and the theorems proved in Appendix A below lead to

$$(2q+1)\partial_+ \psi_{q,p} = \psi_{q-1,p+1} + \psi_{q+1,p+1}. \quad (30)$$

In the same manner, one has

$$\partial_0 r = \cos\theta, \quad (31a)$$

$$\partial_0 \cos\theta = \sin^2\theta / r, \quad (31b)$$

$$\partial_0 \varphi = 0. \quad (31c)$$

Then

$$\begin{aligned} \partial_0 \psi_{q,p} &= \frac{dz_q(r)}{dr} \cos\theta P_q^p(\cos\theta) e^{ip\varphi} \\ &\quad + \frac{z_q(r)}{r} \sin^2\theta \frac{dP_q^p(\cos\theta)}{d\cos\theta} e^{ip\varphi}. \end{aligned} \quad (32)$$

The same recurrence relations between the Bessel functions and the relations given in Appendix A

lead to

$$\begin{aligned} (2q+1)\partial_0 \psi_{q,p} &= (q+p)\psi_{q-1,p} \\ &\quad - (q-p+1)\psi_{q+1,p}. \end{aligned} \quad (33)$$

Consider now both Cartesian frames separated by a distance a as shown in Fig. 1. One has [Eqs. (10.1.45) and (10.1.46) in Ref. 18]

$$\begin{aligned} z_0(r_2) &= \sum_{q=0}^{\infty} (2q+1) z_q(a) j_q(r_1) \\ &\quad \times P_q(\cos\theta_1), \quad r_1 < a. \end{aligned} \quad (34)$$

For the definition of the parameters, see Fig. 1. We may apply the operator $\partial_+^m (m \geq 0)$ on each side of Eq. (34). Using Eq. (30), Eq. (10.1.19) in Ref. 18, and the fact that

$$\psi_{q,m} = 0 \quad q < m, \quad (35)$$

one obtains after some algebra

$$\psi_{m,m}(2) = (2m-1)!! \sum_{q=m}^{\infty} (2q+1) \frac{z_q(a)}{a^m} \psi_{q,m}(1). \quad (36)$$

The variables (1) or (2) indicate that the functions are described in the frame (1) or (2). The Bessel function j_q must be employed in $\psi_{q,m}(1)$. Equation (36) is similar to that obtained by Langbein [Eq. (5.65) in Ref. 24]. Suppose now that one writes

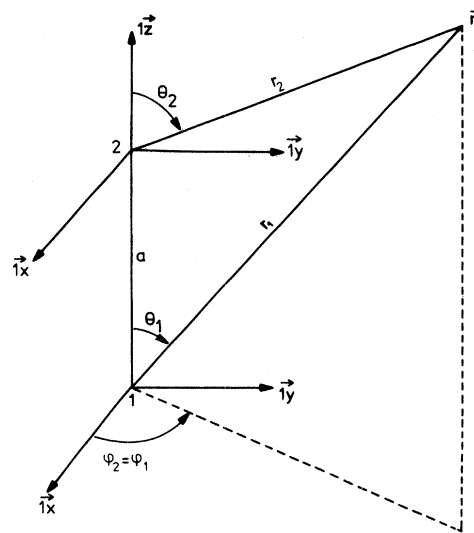


FIG. 1. Reference frame 1 and 2 with position vectors \vec{r}_1 and \vec{r}_2 for an arbitrary point \vec{r} characterized by angles φ and θ_1 , or θ_2 .

$$\psi_{n,m}(2) = \sum_{q=m}^{\infty} (2q+1) \frac{(q-m)!}{(q+m)!} \mathcal{L}_{n,q}^m(a) \psi_{q,m}(1). \tag{37}$$

By comparing Eqs. (37) and (36), we have

$$\mathcal{L}_{m,q}^m(a) = (2m-1)!! \frac{(q+m)!}{(q-m)!} \frac{z_q(a)}{a^m}, \tag{38}$$

which will serve as the initial values for the recurrence.

In order to obtain the recurrence equation, let us apply the operator ∂_0 to both sides of Eq. (37).

After using Eq. (32), one obtains

$$(n+m)\psi_{n-1,m}(2) - (n-m+1)\psi_{n+1,m}(2) = (2n+1) \sum_{q=m}^{\infty} \frac{(q-m)!}{(q+m)!} \times \mathcal{L}_{n,q}^m(a) [(q+m)\psi_{q-1,m}(2) - (q-m+1)\psi_{q+1,m}(2)] \tag{39}$$

Replacing $\psi_{n\pm 1,m}(2)$ by their expressions taken from (37) and comparing the coefficients of $\psi_{q,m}(2)$, one obtains without any difficulty the following recurrence relation:

$$(n-m+1)\mathcal{L}_{n+1,q}^m(a) = (n+m)\mathcal{L}_{n-1,q}^m(a) + \frac{2n+1}{2q+1} [(q+m)\mathcal{L}_{n,q-1}^m(a) - (q-m+1)\mathcal{L}_{n,q+1}^m(a)]. \tag{40}$$

This recurrence relation for what we suggest to call the Langbein function $\mathcal{L}_{n,q}^m(a)$, has for its solution the expression (5.69) in Ref. 24 with an extra factor $(-1)^{n-m}$ due to our choice in the orientation of the reference frames. The above recurrence relation is obviously of greater interest in performing numerical work than Eq. (5.68) of Ref. 24. The numerical work is further facilitated by the fact that

$$\mathcal{L}_{n,q}^m(a) = (-1)^{n+q} \mathcal{L}_{q,n}^m(a). \tag{41}$$

The “vector potential” $\vec{\Gamma}\psi_{qp}$ can now be transposed from frame to frame according to the number of spheres in the system. It was given by Langbein.²⁴ However, rather than using Legendre functions we prefer spherical harmonics, and write

$$\vec{m}_{nm3}(2) = \sum_{q=m}^{\infty} [V_{nq}^m(a)\vec{m}_{qm1}(1) + W_{nq}^m(a)\vec{n}_{qm1}(1)], \tag{42a}$$

and from Eqs. (3a) and (3b)

$$\vec{n}_{nm3}(2) = \sum_{q=m}^{\infty} [W_{nq}^m(a)\vec{m}_{qm1}(1) + V_{nq}^m(a)\vec{n}_{qm1}(1)] \tag{42b}$$

with

$$V_{n,q}^m(a) = A_{n,q}^m \left[q(q+1)\mathcal{L}_{n,q}^m(a) - \frac{q(q-m+1)}{2q+1} a \mathcal{L}_{n,q+1}^m(a) - \frac{(q+1)(q+m)}{2q+1} a \mathcal{L}_{n,q-1}^m(a) \right] \tag{43a}$$

$$W_{n,q}^m(a) = -imA_{n,q}^m \mathcal{L}_{n,q}^m(a)a \tag{43b}$$

where

$$A_{n,q}^m = \left[\frac{(2n+1)(2q+1)}{q(q+1)n(n+1)} \frac{(n-m)!}{(n+m)!} \frac{(q-m)!}{(q+m)!} \right]^{1/2}. \tag{44}$$

Moreover, since

$$Y_{n,-m}(\theta,\varphi) = Y_{n,m}^*(\theta,\varphi)(-1)^m, \tag{45}$$

we have

$$V_{n,q}^{-|m|}(a) = V_{n,q}^{|m|}(a) \tag{46a}$$

$$W_{n,q}^{-|m|}(a) = -W_{n,q}^{|m|}(a). \tag{46b}$$

Equations (46) must be used in order to complete the system for $m < 0$. In Appendix B, the explicit expressions for a few $V_{nq}^m(a)$ and $W_{nq}^m(a)$ are given.

In order to find the interaction terms $\mathcal{T}_{aplm}(i,j)$ and $\mathcal{C}_{aplm}(i,j)$ between two general frames, we proceed exactly as in Ref. 1. Consider the frames as shown in Fig. 2. The polar coordinates at the

origin of the i frame are measured in the j frame and are $(a_{ji}, \alpha_{ji}, \beta_{ji})$. Both systems are rotated around the $\vec{1}_z$ axis by the same angle β_{ji} , then around the new $\vec{1}_y$ axis by the same angle α_{ji} . The final frames (1 and 2) have, then, a common $\vec{1}_z$ axis (as on Fig. 1). By application of Jeffreys theorem,^{1,25} one finally has

$$\xi_{lm}(j) = e^{im\beta_{ji}} \sum_{\nu=-n}^{+n} O(l, m, \nu, \alpha_{ji}) \xi_{l\nu}(1), \quad (47a)$$

$$\xi_{qp}(i) = e^{ip\beta_{ji}} \sum_{\lambda=-q}^{+q} O(q, p, \lambda, \alpha_{ji}) \xi_{q\lambda}(2), \quad (47b)$$

with

$$O(l, m, \nu, \alpha) = (-1)^{l+\nu} [(l+m)!(l-m)!(l+\nu)!(l-\nu)!]^{1/2} \\ \times \sum_{r=f}^g \frac{(-1)^r [\cos(\alpha/2)]^{2r+m+\nu} [\sin(\alpha/2)]^{2(l-r)-m-\nu}}{r!(l-m-r)!(l-\nu-r)!(m+\nu+r)!}, \quad (48)$$

where $f = \max(0, -m-\nu)$ and $g = \min(l-\nu, l-m)$.

Applying the operator $(\vec{\nabla}_\times)^s \vec{r}$, $s=1,2$ to relations (47), one obtains the projections of the functions \vec{m} and \vec{n} as defined in Eq. (3), i.e.,

$$\langle \vec{m}_{qp3}(i) | \vec{m}_{lm1}(j) \rangle = e^{i(p-m)\beta_{ji}} \sum_{\lambda=-q}^{+q} \sum_{\nu=-n}^{+n} O(q, p, \lambda, \alpha_{ji}) O(l, m, \nu, \alpha_{ji}) \langle \vec{m}_{q\lambda3}(2) | \vec{m}_{l\nu1}(1) \rangle \quad (49)$$

and similar relations for the other terms. Using relation (41) for both frames with a common $\vec{1}_z$ axis, and definitions (18), one finally obtains

$$\mathcal{T}_{qplm}(i, j) = e^{i(p-m)\beta_{ji}} \sum_{\lambda=-d}^{+d} O(q, p, \lambda, \alpha_{ji}) \\ \times O(l, m, \lambda, \alpha_{ji}) \\ \times V_{q,l}^\lambda(ka_{ji}) \quad (50a)$$

$$\mathcal{C}_{qplm}(i, j) = e^{i(p-m)\beta_{ji}} \sum_{\lambda=-d}^{+d} O(q, p, \lambda, \alpha_{ji}) \\ \times O(l, m, \lambda, \alpha_{ji}) \\ \times W_{q,l}^\lambda(ka_{ji}) \quad (50b)$$

with $d = \min(q, l)$. The wave number k has been reintroduced here for clarity. Notice a fundamental difference with the nonretarded case¹: it is in general not possible to write the interaction terms as a separable product between the distance and the angular-dependent terms. Relations (50) complete the Eqs. (21) in order to solve the problem of interaction between arbitrarily polarizable spheres embedded in an infinite matrix and submitted to a given incident wave.

D. The incident wave

The case of a plane polarized wave only, is considered here. It is first convenient to calculate the coefficients of the expansion (19) for a wave vector \vec{k} parallel to the $\vec{1}_z$ axis of a frame O_j' centered on the j sphere. We choose this frame $(\vec{1}_{x'}, \vec{1}_{y'}, \vec{1}_{z'})$ such that

$$\vec{E}_0 = E_0 e^{ikr \cos\theta + i\vec{k} \cdot \vec{u}_j} \vec{1}_{x'}, \quad (51a)$$

$$\vec{H}_0 = iH_0 e^{ikr \cos\theta + i\vec{k} \cdot \vec{u}_j} \vec{1}_{y'}, \quad (51b)$$

where \vec{u}_j is the position of the sphere in the gen-

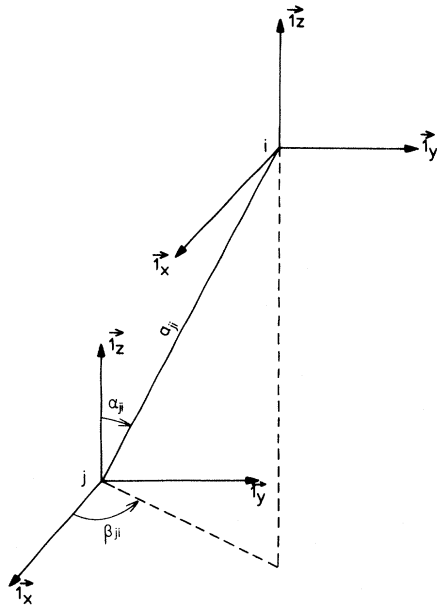


FIG. 2. Polar coordinates $(a_{ji}, \alpha_{ji}, \beta_{ji})$ for the i -reference frame in the j -reference frame.

eral reference frame O for which the axes are in general not parallel to those of the frame O'_j . The spherical coordinates of a point \vec{r} are $(r'_j, \theta'_j, \varphi'_j)$ and are given in the frame O'_j . Comparing Eqs. (51) with Eq. (19) and using the orthogonality of the functions \vec{m}_{nm} and \vec{n}_{nm} , one has

$$a'_{nm}(j) = e^{i\vec{k}\cdot\vec{u}_j} \frac{\int \int e^{ikr \cos\theta} \vec{1}_{x'} \cdot \vec{m}_{nm}^* d\Omega'_j}{\int \int |\vec{m}'_{nm1}|^2 d\Omega'_j}, \quad (52a)$$

$$b'_{nm}(j) = ie^{i\vec{k}\cdot\vec{u}_j} \frac{\int \int e^{ikr \cos\theta} \vec{1}_{y'} \cdot m_{nm}^* d\Omega'_j}{\int \int |\vec{m}'_{nm1}|^2 d\Omega'_j}, \quad (52b)$$

where the prime denotes here that the coefficients and functions are described in the frame O'_j . Equation (10.1.47) in Ref. 18 gives

$$e^{ikr \cos\theta} = \sum_{q=0}^{\infty} i^q [4\pi(2q+1)]^{1/2} j_q(kr) Y_{q0}(\theta, \varphi). \quad (53)$$

Using the expression (2a) for the \vec{n}_{nm1} , it is quite easy to obtain by direct integration

$$a'_{nm}(j) = e^{i\vec{k}\cdot\vec{u}_j} i^{n+1} [\pi(2n+1)]^{1/2} \delta_{m, \pm 1}, \quad (54a)$$

$$b'_{nm}(j) = e^{i\vec{k}\cdot\vec{u}_j} m i^{n+1} [\pi(2n+1)]^{1/2} \delta_{m, \pm 1}, \quad (54b)$$

$$a_{nm}^I(j) = i^{n+1} [\pi(2n+1)]^{1/2} e^{-im\beta} [e^{-i\gamma} O(n, 1, m, -\alpha) + e^{i\gamma} O(n, -1, m, -\alpha)] e^{i\vec{k}\cdot\vec{u}_j} \quad (56a)$$

$$b_{nm}^I(j) = i^{n+1} [\pi(2n+1)]^{1/2} e^{-im\beta} [e^{-i\gamma} O(n, 1, m, -\alpha) - e^{i\gamma} O(n, -1, m, -\alpha)] e^{i\vec{k}\cdot\vec{u}_j}. \quad (56b)$$

Equations (56) allow one to study the effect of different angles of incidence of the wave without having each time to rotate the system of the spheres. Therefore the interaction matrices \mathcal{L} and \mathcal{Z} , which in fact depend on the geometry, are the same for any incident wave, and only the independent vectors \vec{l} and \vec{a} are changing. Computer work is thus necessarily reduced and much more easy.

E. The extinction cross section

In order to calculate observed spectra, it is useful to calculate either the energy absorbed or diffracted by the spheres, or the sum of both energies. The Poynting vector is given by¹⁶

$$\vec{S} = \frac{1}{2} \vec{E}_M \times \vec{H}_M^*, \quad (57)$$

where \vec{E}_M and \vec{H}_M are given by Eqs. (15). This

where $\delta_{l,m}$ is the Kronecker symbol.

The wave vector \vec{k} is defined by its polar coordinates (k, α, β) in the O frame. The angle between the magnetic field and the intersection of the plane (\vec{k}, \vec{H}_0) with the horizontal $(\vec{1}_x, \vec{1}_y)$ plane is denoted as γ . In order to express the wave in a frame O_j which has the three axes parallel to the axis $(\vec{1}_x, \vec{1}_y, \vec{1}_z)$ of the general frame O , one makes three successive rotations of the frame O'_j , i.e., (1) rotation around the $\vec{1}'_z$ axis of an angle γ to obtain $(\vec{1}_{x''}, \vec{1}_{y''}, \vec{1}_{z''} = \vec{1}_{z'})$; (2) rotation around the $\vec{1}_{y''}$ axis of an angle α to obtain $(\vec{1}_{x'''}, \vec{1}_{y'''} = \vec{1}_{y''}, \vec{1}_{z'''})$; (3) rotation around the $\vec{1}_{z'''}$ axis of an angle β to obtain $(\vec{1}_x, \vec{1}_y, \vec{1}_z = \vec{1}_{z''''})$.

Using Eqs. (19) and (47a) giving the relation between the functions ξ_{lm} under frame rotation, one has

$$a_{nm}^I(j) = e^{-im\beta} \sum_{\lambda=-n}^{+n} O(n, \lambda, m, -\alpha) e^{-i\lambda\gamma} a_{n\lambda}^I(j), \quad (55)$$

where the $a_{nm}^I(j)$'s are the coefficients of the expansions (19) with respect to the functions \vec{m}_{nm} and \vec{n}_{nm} calculated in the O_j frame. The same relation holds for the $b_{nm}^I(j)$. Hence, following Eq. (54),

vector clearly contains

$$\vec{S} = \frac{1}{2} \vec{E}_0 \times \vec{H}_0^* + \frac{1}{2} \left[\sum_{j=1}^N \vec{E}_0 \times \vec{H}_D^*(j) + \sum_{j=1}^N \vec{E}_D(j) \times \vec{H}_0^* \right] + \frac{1}{2} \sum_{l=1}^N \sum_{j=1}^N \vec{E}_D(j) \times \vec{H}_D^*(l), \quad (58)$$

where $\vec{H}_D(j)$ and $\vec{E}_D(j)$ are the fields diffracted by the j sphere. In order to calculate the energy, one integrates the normal component of the Poynting vector on a large sphere containing all the particles, i.e., respectively,

$$W_a = -\text{Re} \int \int \vec{S} \cdot \vec{1} da, \quad (59)$$

$$W_t = -\frac{1}{2} \text{Re} \int \int \left[\sum_{j=1}^N \vec{E}_0 \times \vec{H}_D^*(j) + \sum_{j=1}^N \vec{E}_D(j) \times \vec{H}_0^* \right] \cdot \vec{1}_r da, \quad (60)$$

$$W_s = \frac{1}{2} \text{Re} \int \int \sum_{l=1}^N \sum_{j=1}^N [\vec{E}_D(j) \times \vec{H}_D^*(l)] \cdot \vec{1}_r da, \quad (61)$$

$$W_0 = \frac{1}{2} \text{Re} \int \int [\vec{E}_0 \times \vec{H}_0^*] \cdot \vec{1}_r da, \quad (62)$$

where W_a (W_s) is the power absorbed (scattered) by the particles, W_0 is power dissipated by the incident wave, and W_t is the total power of the system

$$W_t = W_0 + W_s + W_a. \quad (63)$$

Because of the coupling between fields diffracted by the various spheres, it is quite difficult to calculate W_s . The final expression for this quantity is more complicated than the "classical" form¹⁶ for a single particle and is not very useful. W_0 , on the other hand, vanishes when the incident wave is a plane wave created in a nondissipative matrix (e.g., k real). W_t can be easily calculated in this case. In order to obtain W_s , one may calculate W_a by integrating the Poynting vector on the surface of all the spheres, and using Eq. (63).

However, in order to compare our calculation on aggregation effects with the results of Ruppin¹⁵ for a single sphere, it is only necessary to calculate W_t and obtain a simple expression for the extinction cross section. We replace the fields in Eq. (60) by their developments in terms of functions \vec{m}_{nm} and \vec{n}_{nm} . From Eqs. (15), one has

$$\vec{E}_D(j) = E_0 \sum_{q,p} [c_{qp}^M(j) \vec{m}_{qp3}(j) + d_{qp}^M(j) \vec{n}_{qp3}(j)] \quad (64a)$$

$$\vec{H}_D(j) = H_0 \sum_{q,p} [d_{qp}^M(j) \vec{m}_{qp3}(j) + c_{qp}^M(j) \vec{n}_{qp3}(j)]. \quad (64b)$$

The incident fields are expressed in terms of functions \vec{m} and \vec{n} calculated in the frame centered on the j sphere [Eqs. (19)]. We then use the properties (2) to calculate the following integrals:

$$\int \int (\vec{m}_{nm} \times \vec{m}_{qp}^*) \cdot \vec{1}_r d\Omega = \int \int (\vec{n}_{nm} \times \vec{n}_{qp}^*) \cdot \vec{1}_r d\Omega = 0, \quad (65)$$

$$\int \int (\vec{m}_{nm1} \times \vec{n}_{qp3}^*) \cdot \vec{1}_r d\Omega = \frac{j_n(kr)}{kr} [kr h_n^{(1)}(kr)]^* \times \delta_{q,n} \delta_{m,p}, \quad (66)$$

and similarly for the other products. The calculation of Eqs. (65), (66), and the other terms make use of the following orthogonality relations:

$$\int \int \left[\frac{dY_{nm}}{d\theta} \frac{dY_{qp}^*}{d\theta} + mp \frac{Y_{nm} Y_{qp}^*}{\sin^2 \theta} \right] d\Omega = n(n+1) \delta_{q,n} \delta_{m,p}, \quad (67)$$

$$\int \int \left[p \frac{dY_{nm}}{d\theta} \frac{Y_{qp}^*}{\sin \theta} + m \frac{dY_{qp}^*}{d\theta} \frac{Y_{nm}}{\sin \theta} \right] d\Omega = 0, \quad (68)$$

where the Y_{nm} 's are abbreviations for the $Y_{nm}(\theta, \varphi)$'s.

When r tends to infinity, the usual asymptotic expansions of Bessel functions are

$$j_n(kr) \sim \sin(kr - n\pi/2)/kr \quad (69)$$

$$h_n^{(1)}(kr) \sim i^{-n-1} e^{ikr}/kr. \quad (70)$$

Because k is real, we finally obtain after insertion of Eqs. (69), (70), (64), (65), (66), (19), and (6a) into (60):

$$W_t = -\frac{1}{2k^2} \left[\frac{\epsilon}{\mu} \right]^{1/2} E_0^2 \sum_{j=1}^N \sum_{n,m} \text{Re} [a_{nm}^{I*}(j) c_{nm}^M(j) + b_{nm}^{I*}(j) d_{nm}^M(j)]. \quad (71)$$

The extinction cross section σ_e (measured in units of the total section $\pi \sum_{j=1}^N R_j^2$ of the spheres) is obtained from the ratio of the power W_t to the power flow per unit area of the incident wave, i.e., for an incident plane wave

$$\sigma_e = \frac{-1}{\pi \sum_j (kR_j)^2} \sum_{j=1}^N \sum_{n,m} \text{Re} [a_{nm}^{I*}(j) c_{nm}^M(j) + b_{nm}^{J*}(j) d_{nm}^M(j)] \quad (72)$$

which generalizes Eq. (27) given by Ruppin.¹⁵

III. EXAMPLES: METALLIC SPHERES

One of our aims is to show how the spectra obtained in the case of isolated metallic spheres are modified by the interactions between various spheres. This necessarily implies the choice of some particular aggregate for which the extinction cross section is calculated. In this paper, we present results for a two-sphere cluster and for an

infinite linear chain of identical particles. Retardation effects are very sensitive when the value of the wave vector k is finite, i.e., when the characteristic quantity ka is not negligible compared to unity (a is the distance between the centers of two neighboring spheres). For comparison to Ruppin,¹⁵ the dielectric constants are taken to be by

$$\epsilon^T(k, \omega) = 1 - \frac{1}{x(x+i\rho)} \frac{3}{2y^2} \left[\frac{1+y^2}{y} \tan^{-1}y - 1 \right] \quad (73)$$

$$\epsilon^L(k, \omega) = 1 - \frac{1}{x(x+i\rho)} \frac{3}{y^2} \left[1 - \frac{\tan^{-1}y}{y} \right] \times \left[1 + \frac{i\rho}{x} \left[1 - \frac{\tan^{-1}y}{y} \right] \right]^{-1}, \quad (74)$$

where

$$y^2 = \frac{-k^2 v_F^2}{\omega_p^2(x+i\rho)} \quad (75)$$

$$x = \omega/\omega_p \quad (76)$$

in which ω_p is the plasma frequency, ρ the complex damping factor, and v_F the Fermi velocity.

Using for sodium spheres the values $\omega_p = 8.65 \times 10^{15} \text{ sec}^{-1}$, $v_F = 1.07 \times 10^6 \text{ m/sec}$, and

$$\rho = \rho_0 + \eta(k^L/k^F)^2, \quad (77)$$

where k^F is the Fermi wave number,^{15,26,27} we let $\rho_0 = 0.01$ and $\eta = 0.05$. The transverse and the longitudinal wave numbers k^T and k^L are, respectively, solutions of the implicit equations (6a) and (6b), where the magnetic permeability of the spheres μ_s is used. Here we take^{15,28} $\mu_s = 1$ or 0.75. Longitudinal plasmon effects are quite important when the spheres are very small, since their propagation is then in the whole volume. Hence in the following examples we have taken radii smaller than 60 Å. The matrix is supposed to be the vacuum ($\epsilon = \mu = 1$).

A. The two-sphere cluster

If we place the two centers on the $\vec{1}_z$ axis, Eqs. (21) may be separated according to the index m . The sum is limited in the left-hand side to $q = 1$. Using the symmetry properties of the \mathcal{S} and \mathcal{C} terms, the following matrix equations are easily derived:

$$\begin{bmatrix} 1 & -\Gamma_1(1)V_{11}^0(ka) \\ -\Gamma_1(2)V_{11}^0(ka) & 1 \end{bmatrix} \begin{bmatrix} e_{10}(1) \\ e_{10}(2) \end{bmatrix} = \begin{bmatrix} \Gamma_1(1)\alpha_{10} \\ \Gamma_1(2)\alpha_{10}e^{i\vec{k}\cdot\vec{a}} \end{bmatrix} \quad (78a)$$

and

$$\begin{bmatrix} 1 & -\Delta_1(1)V_{11}^0(ka) \\ -\Delta_1(2)V_{11}^0(ka) & 1 \end{bmatrix} \begin{bmatrix} \mathcal{L}_{10}(1) \\ \mathcal{L}_{10}(2) \end{bmatrix} = \begin{bmatrix} \Delta_1(1)\mathcal{L}_{10} \\ \Delta_1(2)\mathcal{L}_{10}e^{i\vec{k}\cdot\vec{a}} \end{bmatrix} \quad (78b)$$

since $W_{11}^0(ka) = 0$. For $m = \pm 1$, the systems are not separable into purely magnetic and purely electric parts, but lead to a set of four equations, i.e.,

$$\begin{bmatrix} 1 & -V_{11}^1(ka)\Delta_1(1) & 0 & \mp W_{11}^1(ka)\Delta_1(1) \\ -V_{11}^1(ka)\Delta_1(2) & 1 & \pm W_{11}^1(ka)\Delta_1(2) & 0 \\ 0 & \mp W_{11}^1(ka)\Gamma_1(1) & 1 & -V_{11}^1(ka)\Gamma_1(1) \\ \pm W_{11}^1(ka)\Gamma_1(2) & 0 & -V_{11}^1(ka)\Gamma_1(2) & 1 \end{bmatrix} \begin{bmatrix} \mathcal{L}_{1,\pm 1}^M(1) \\ \mathcal{L}_{1,\pm 1}^M(2) \\ e_{1,\pm 1}^M(1) \\ e_{1,\pm 1}^M(2) \end{bmatrix} = \begin{bmatrix} \mathcal{L}_{1,\pm 1}^I \\ \mathcal{L}_{1,\pm 1}^I e^{i\vec{k}\cdot\vec{a}} \\ \alpha_{1,\pm 1}^I \\ \alpha_{1,\pm 1}^I e^{i\vec{k}\cdot\vec{a}} \end{bmatrix}, \quad (79)$$

where the upper (lower) sign is used for $m = +1$ (-1). The \mathcal{L} 's and the α 's are given by Eqs. (56) without the position-dependent factor $e^{i\vec{k}\cdot\vec{u}_j}$ which is explicitly written in Eqs. (78) and (79). The vector \vec{a} is the vector joining the center of the sphere 1 to the center of the sphere 2.

B. The linear chain

The linear infinite chain of identical particles is of interest because it gives an idea on the behavior of regular and random distribution of spheres by suggesting boundary limits of spectra.¹¹ The dis-

tance between two neighboring centers is denoted by a . Applying the Bloch theorem to the definition of the field coefficients, i.e.,

$$c_{nm}^M(j) = c_{nm}^M e^{i\vec{q} \cdot \vec{u}_j}, \quad (80a)$$

$$d_{nm}^M(j) = d_{nm}^M e^{i\vec{q} \cdot \vec{u}_j}, \quad (80b)$$

where \vec{q} is a wave number, and rewriting Eqs. (21), it is easy to show that solutions of (80) can exist

only if $\vec{q} = \vec{k}$. Thus only the modes with the same wave number as that of the incident wave are excited. The equations including the dipole-dipole interaction only [i.e., $q \leq 1$ in the sum of Eqs. (21)] are solved to find c_{1m}^M and d_{1m}^M which are substituted into Eq. (72) for the extinction cross section σ_e . Using expressions (56) for the coefficients of the expansion of the incident beam, we obtain after some algebra

$$\sigma_e = -\frac{6}{(kR)^2} \operatorname{Re} \left[\sin^2 \alpha \left(\frac{\Gamma_1}{1 - I_{11}^0 \Gamma_1} \sin^2 \gamma + \frac{\Delta_1}{1 - I_{11}^0 \Delta_1} \cos^2 \gamma \right) + \frac{\Gamma_1(1 - \sin^2 \alpha \sin^2 \gamma) + \Delta_1(1 - \sin^2 \alpha \cos^2 \gamma) + (\sin^2 \alpha - 2)I_{11}^1 \Gamma_1 \Delta_1 + 2 \cos \alpha C_{11}^1 \Delta_1 \Gamma_1}{(1 - I_{11}^1 \Gamma_1)(1 - I_{11}^1 \Delta_1) - (C_{11}^1)^2 \Gamma_1 \Delta_1} \right] \quad (81)$$

where (using the properties of symmetry for the \mathcal{S} and \mathcal{C})

$$I_{11}^m = 2 \sum_{n=1}^{\infty} \cos(nka \cos \alpha) V_{11}^m(nka), \quad m = 0, 1 \quad (82)$$

$$C_{11}^1 = 2i \sum_{n=1}^{\infty} \sin(nka \cos \alpha) W_{11}^1(nka). \quad (83)$$

Using the explicit expression for V_{11}^m and W_{11}^1 given in Appendix B, those coefficients are

$$I_{11}^0 = [-3/(ka)^2] \{ S_2(x^+) + S_2(x^-) + i[S_3(x^+) + S_3(x^-)]/ka \}, \quad (84)$$

$$I_{11}^1 = [-3i/(2ka)] \{ S_1(x^+) + S_1(x^-) + i[S_2(x^+) + S_2(x^-)]/ka - [S_3(x^+) + S_3(x^-)]/(ka)^2 \}, \quad (85)$$

$$C_{11}^1 = [3i/(2ka)] \{ S_1(x^+) - S_1(x^-) + i[S_2(x^+) - S_2(x^-)]/ka \}, \quad (86)$$

where

$$x^\pm = ka(1 \pm \cos \alpha) \quad (87)$$

$$S_n(z) = \sum_{l=1}^{\infty} \frac{e^{ilz}}{l^n}. \quad (88)$$

The sums are calculated numerically for $n \geq 2$. In the case $n = 1$, formulas (1.441) in Ref. 29 give

$$S_1(z) = -\frac{1}{2} \{ \ln[2(1 - \cos \bar{z})] - i(\pi - \bar{z}) \}, \quad (89)$$

where \bar{z} is the value of z restricted to the interval $(0, 2\pi)$. Notice that the terms I_{11}^1 and C_{11}^1 do not converge when

$$\cos \alpha = 2l\pi/ka \pm 1 \quad (90)$$

where l is an integer.

The complete analysis of this divergence is outside the scope of this paper.³⁰ One of the main conclusions is that $\sigma_e = 0$ when $\alpha = 0$ or $\alpha = \pi$ and $k \neq 0$. This corresponds to the situation of a beam

along the axis of the chain. When relation (90) holds, σ_e is nonzero in the general case $l \neq 0$.

IV. NUMERICAL RESULTS

We successively consider the case of two interacting metallic spheres, and that of the linear chain. We investigate the dependence of the optical properties on some of the physical parameters characterizing spherule ensembles and their surrounding, i.e., size and relative size effect, separation effect, magnetic permeability effect, and some matrix property effect.

Since the spectra depend on the angle of incidence of the light when the clusters have a symmetry axis, let us define the scattering geometry. The light-wave vector can be either parallel, perpendicular, or at an oblique incidence to the vector joining the sphere centers. An arbitrary incidence complicates the discussion of numerical results.

The case of the wave vector parallel to the $\vec{1}_z$ axis is not considered here because it induces shadow effects which need a special analysis. Therefore, only two simple cases are considered here (Fig. 3). In both cases the wave vector \vec{k} is set to be in the $\vec{1}_x$ direction. The case when the incident electric field is parallel to the $\vec{1}_z$ axis will be denoted by E_{\parallel} , and the case when it is perpendicular to the $\vec{1}_z$ axis by E_{\perp} . Field and resonance equations can be simplified for these cases, but a general computer program was explicitly written. Let us nevertheless recall that only a few coefficients (a, b, c, d labeled by m) in Eq. (71) must be calculated, since several of them vanish according to the mode index m and the field geometry. Comparison to the classical Mie theory is not made here, since it was discussed by Ruppin¹⁵ in the case of isolated spheres, but comparison to Ruppin results is relevant.

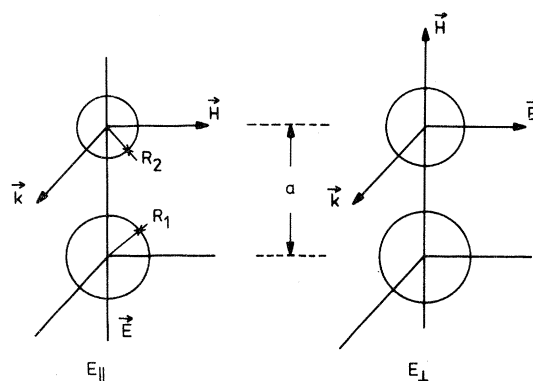


FIG. 3. Geometry of the incident plane wave ($\vec{E}, \vec{H}, \vec{k}$) with respect to the symmetry axis of the binary cluster (or of the infinite linear chain by mere replication). The \vec{k} vector is always perpendicular to the chain, but the electric field is perpendicularly (E_{\perp}) polarized or is parallel (E_{\parallel}) to the axis.

A. Two-sphere cluster

1. Size effect

Consider first the case of the binary cluster with two identical Na spheres (radii $R_1 = R_2 = 15 \text{ \AA}$ as

in Ref. 15) in contact. The permeability of the spheres is chosen equal to unity.¹⁵ The calculated extinction cross section in units of the total geometric section is shown in Fig. 4 in both cases

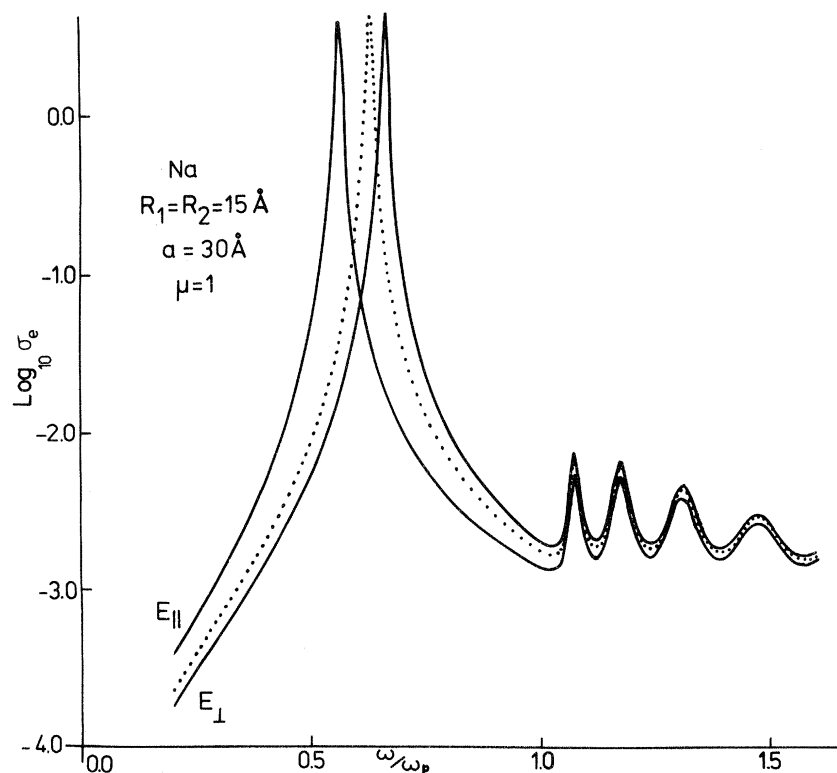


FIG. 4. Logarithm of the extinction cross section σ_e for the binary sphere cluster of two equal-sized ($R_1 = R_2 = 15 \text{ \AA}$) sodium spheres for a separation of spheres $a = R_1 + R_2 = 30 \text{ \AA}$ ($\mu = 1$) in an incident-plane polarized wave (E_{\perp} and E_{\parallel}). The dotted line corresponds to the noninteracting case (Ref. 15).

($E_{||}$ and E_{\perp}) as a function of the ratio ω/ω_p . Clearly, the angle of incidence plays a dramatic role on the main resonance peak position. The dotted line is the Ruppin result for a single sphere. The peaks amplitudes are equivalent, but the shift magnitude is noticeably geometry dependent. Let us recall that this main peak is due to resonance excitation of the transverse electromagnetic mode in the cluster. In the E_{\perp} geometry, the excitation is, of course, "stiffer" to induce. On the other hand, the plasmon peaks occur at approximately the same frequencies as those of isolated spheres, but their amplitudes are modified.

These results are easily interpreted as follows. Consider the determinant of the matrices appearing in Eqs. (78) and (79). The $m=0$ modes are obtained from the calculation of the minimum of the absolute value of $1-[V_{11}^0\Delta_1]^2$ or $1-[V_{11}^0\Gamma_1]^2$, with $\Delta_1(1)=\Delta_1(2)=\Delta_1$ (and the same for Γ_1), while the $m=\pm 1$ modes arises at the minimum of the absolute value of

$$[1-(V_{11}^1\Delta_1)^2][1-(V_{11}^1\Gamma_1)^2] + 2(W_{11}^1)^2\Delta_1\Gamma_1[1-(V_{11}^1)^2\Delta_1\Gamma_1]. \quad (91)$$

Therefore, when $W_{11}^1\Gamma_1$ is small (as here), the main resonance occurs near $1=(V_{11}^1\Delta_1)^2$ rather than near $\Delta_1\sim\infty$ for the single sphere. Hence an important shift of the steep peak at $\omega=\omega_R$ occurs. But a very mild variation of the peaks at $\omega>\omega_p$ is induced since in such a region Δ_1 is a smooth function. The small peaks thus occur only because of bulk plasmon excitations. This different behavior can also be seen if one notices that the main $m=\pm 1$ term of the extinction cross section can be recast into the form

$$\frac{2\Delta_1}{1-(V_{11}^1\Delta_1)^2}g[\Gamma_1,\Delta_1,V_{11}^1,W_{11}^1] \quad (92)$$

and by observing the behavior of this expression for both limits ($\Delta_1\rightarrow\infty, \Delta_1\rightarrow 1/V_{11}^1$).

Consider next the case of spheres of different radii in contact (a) $R_1=15 \text{ \AA}$, $R_2=30 \text{ \AA}$; (b) $R_1=30 \text{ \AA}$, $R_2=60 \text{ \AA}$. This is a more complex situation in which σ_e markedly deviates from a σ_e averaged for two noninteracting unequal-sized spheres (dotted line, Fig. 5). The scattering geometry is again very relevant and leads to a large variation of the spectrum near the main resonance peak. Two very separate peaks appear in each case. Near $\omega=\omega_R$, the $E_{||}$ spectrum is much broader than the E_{\perp} one. The peak position and corresponding type of excitation can be easily interpreted by considering the

four simplest orientations of two interacting dipoles. From low to high frequency, the peaks correspond to excitations of "longitudinal-acoustic," "transverse-optic," "transverse-acoustic," and "longitudinal-optic" electromagnetic modes. Such a splitting occurs because of the unequal size of the spheres, i.e., in Eq. (92) we replace $2\Delta_1$ by $\Delta_1(1)+\Delta_1(2)$ and Δ_1^2 by $\Delta_1(1)\Delta_1(2)$. Furthermore, it (slowly) increases when the relative surface cross section (and sphere volume) decreases. Notice that on the averaged spectrum (dotted line) of two noninteracting unequal large-sized spheres [Fig. 5(b)], the two-peak structure has disappeared into the resonance peak of the largest sphere.

The small-amplitude plasmon peaks at $\omega>\omega_p$ are numerous since they occur at rather different frequencies. A comment on the displayed amplitude is in order. It is observed [Fig. 5(a)] that such an amplitude is not as smooth (decreasing as on Fig. 4) a function of frequency. This is due to the variation in relative amplitude and periodicity of these peaks as a function of sphere radius. Furthermore, the largest amplitude (third small peak) differs from that of the first small peak on Fig. 4 because of the normalization used in calculating σ_e by Eq. (72). We have chosen to calculate an experimentally more realistic quantity, i.e., a measure of the scattered energy [$W_t(1)=W_t(2)$]/(S_1+S_2), rather than $W_t(1)/S_1+W_t(2)/S_2$, where $W_t(i)$ is the power scattered by the i sphere and S_i is the sphere cross section.

2. Separation effect

We show on Fig. 6 the variation of the extinction spectrum when both sphere centers are separated by various distances a . Radii are $R_1=R_2=15 \text{ \AA}$. The number of peaks is, of course, unchanged with respect to the contact case. The main resonance peak rather quickly merges into that for the isolated spheres [the interaction V_{11}^m decreases here as $1/(ka)^3$], and the variation is barely distinguishable when $a\approx 5R$. The merging of the excited bulk plasmon peaks into those of the noninteracting case is rather rapid. This is an experimental bonus since we thus show *a contrario* how close the spheres can be and yet "not influence" each other. However, the information contained in the light polarization incidence is lost in this "free-sphere" case.

In the case of greater values of ka (for example, if the matrix has a high dielectric permittivity ϵ),

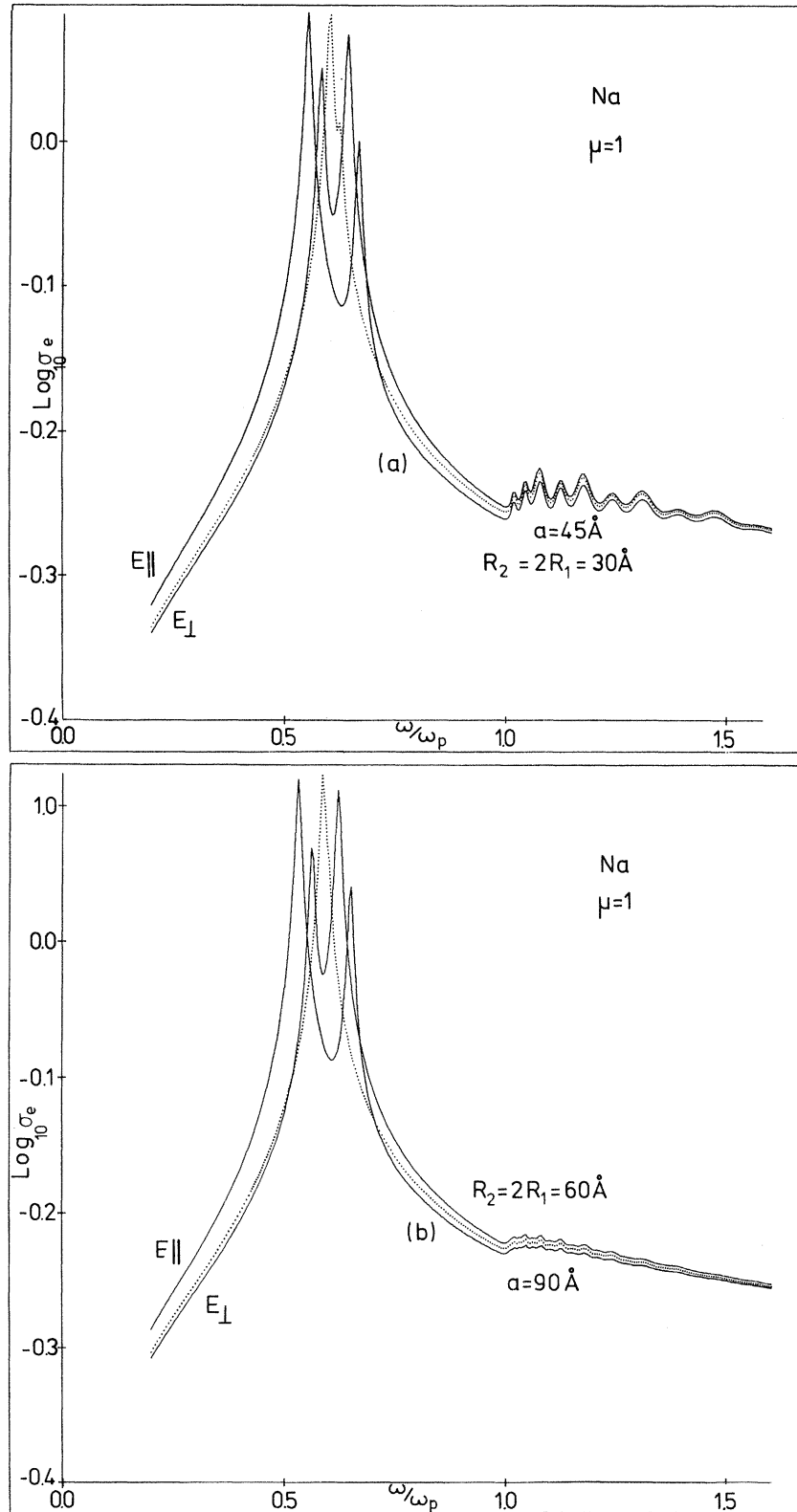


FIG. 5. Logarithm of the extinction cross section σ_e for binary clusters of two unequal-sized sodium spheres with $\mu=1$ in vacuum: (a) $R_1=15\text{ \AA}$, $R_2=30\text{ \AA}$, $a=45\text{ \AA}$, and (b) $R_1=30\text{ \AA}$, $R_2=60\text{ \AA}$, $a=90\text{ \AA}$ as compared to the (averaged) cross section for noninteracting (or isolated) spheres. Polarization geometries of the incident wave are indicated.

the interactions V_{11}^1 decrease as $1/ka$. The main resonance (as a function of the distance) would emerge much more slowly into the peak of the single sphere. This case is not examined here, because the higher multipolar interactions terms are large and will drastically change the spectrum; a dipolar development of the extinction cross section is no longer valid in such a case.

On Fig. 7, we show the more realistic case of two separate unequal-sized sphere extinction cross sections ($R_1=15 \text{ \AA}$, $R_2=30 \text{ \AA}$) the number of peaks is unchanged, and the double-peak structure is conserved even for rather large distances a . This is due, of course, to the radius dependence of the electromagnetic mode frequency for a single sphere. On the other hand, the light incidence effect on the main peak remains, although it is much attenuated. The effect is weak on the plasmon peaks. The same behavior is observed following an increase in radius size [Fig. 7(b): $R_1=30 \text{ \AA}$, $R_2=60 \text{ \AA}$].

3. Magnetic permeability effect

For the above calculation, the magnetic permeability of the spheres was chosen as in Ref. 15 to be a constant $\mu=1$. In so doing, the susceptibility $\Gamma_1 \simeq 0$. It seemed interesting to observe the change in the spectrum due to a finite value of Γ_1 . In fact, for bulk sodium, $\mu=0.75$.²⁸ Such a "drastic" change, however, does not lead to any appreciable effect on the spectrum. Indeed, in such a case $|\Gamma_1/(kR)^3| \simeq 0.06$. A magnetic permeability effect would strongly modify the spectrum only if the coupling factor $W_{11}^1 \Gamma_1$ sharply increases. This is discussed in Sec. V.

B. Linear chain

The overall shape of the absorption cross-section curve as a function of frequency does not appreci-

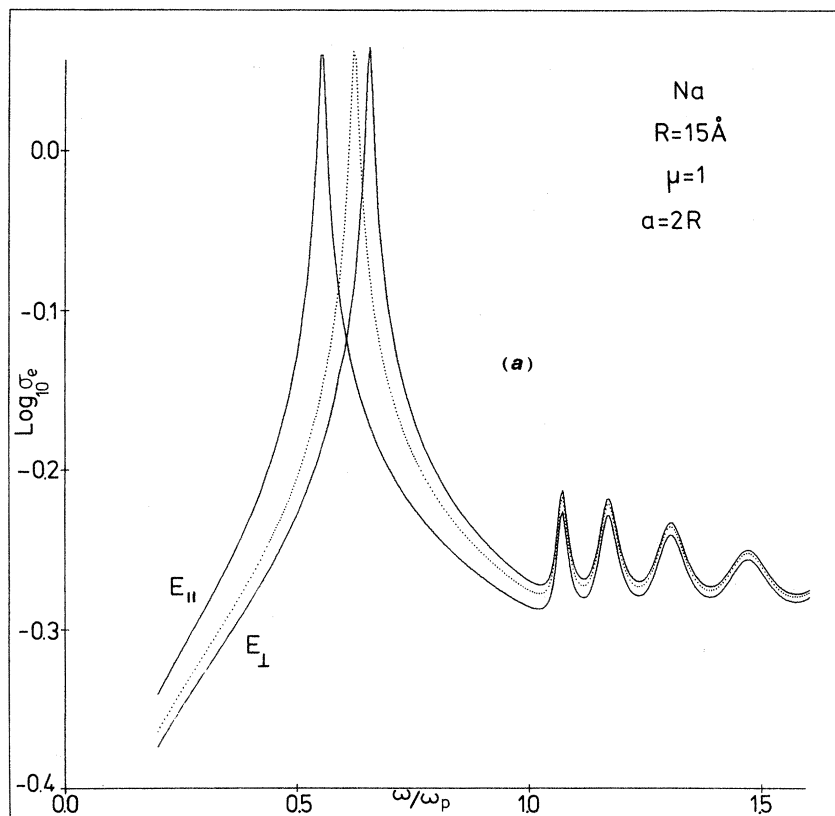


FIG. 6. Logarithm of the extinction cross section σ_e for binary clusters of two equal-sized sodium spheres (with $\mu=1$) in vacuum. The sphere radius is 15 \AA , but the sphere separation a is, respectively, (a) 30 ; (b) 45 ; (c) 60 ; (d) 90 ; (e) 120 \AA . The dotted lines correspond to the case of noninteracting spheres. The field polarization (E_{\perp} or E_{\parallel}) is indicated.

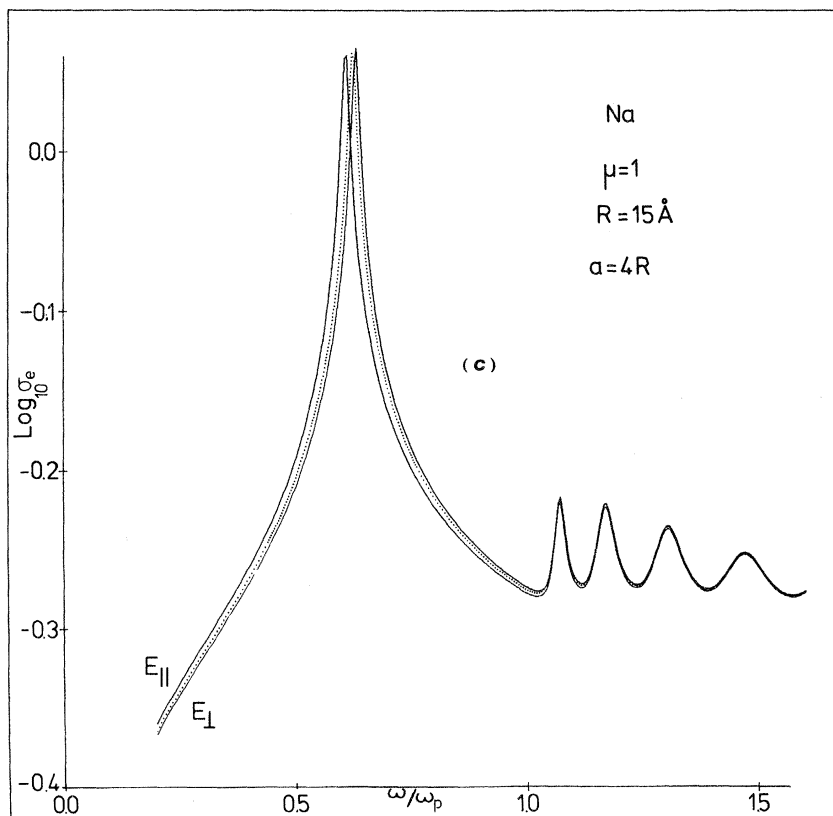
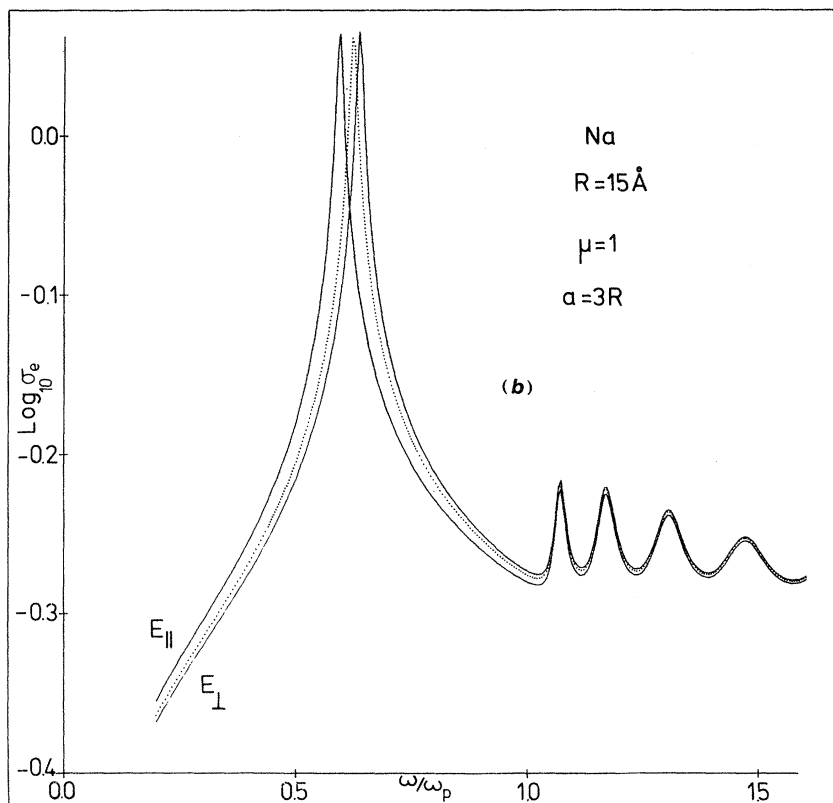


FIG. 6. (Continued.)

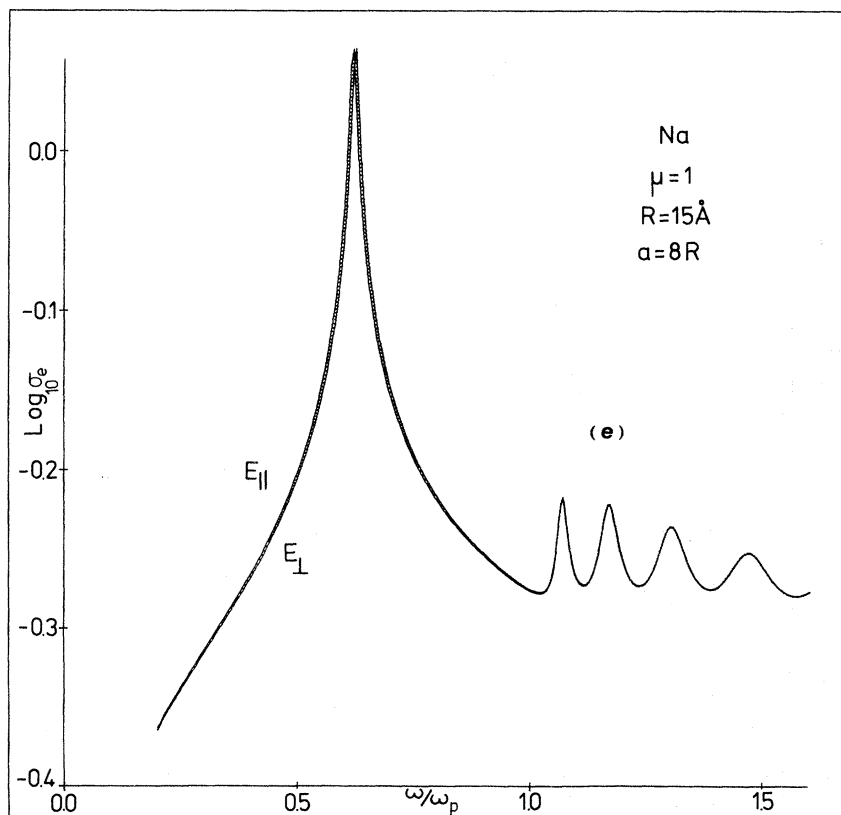
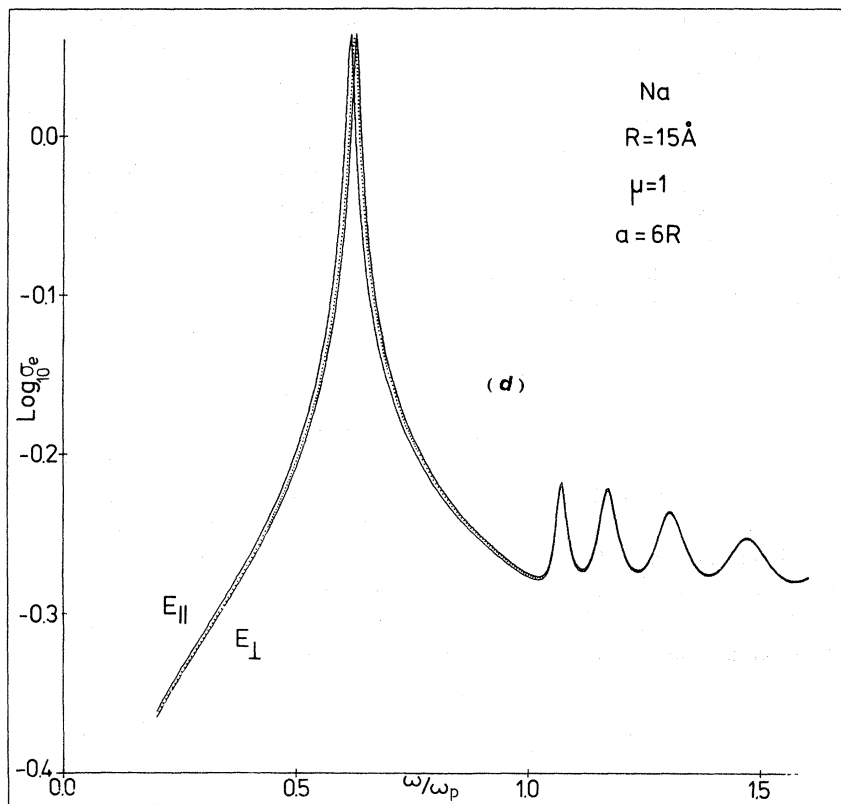


FIG. 6. (Continued.)

ably differ from that seen on Figs. 4–7 for the binary cluster. Therefore a graphical display of such curves seems unnecessary for all parameter changes. A typical example is given on Fig. 8.

Let us note that the main variation is in the amplitude of the small plasmon peaks. The difference between amplitudes for the cases $E_{||}$ and E_{\perp} is much more marked than in the case of the binary cluster, in particular taking into account the fact that the scale is logarithmic. The moderate change in the cross-section amplitude when spheres have unequal radii is also visible (but not shown) when compared to that seen for the unequal-sized-sphere binary cluster (Fig. 5). In general the frequency separation for the main resonance is also larger.

On Fig. 9 we give some indication of such variations. The position of the main resonance is shown as a function of the ratio R/a for the E_{\perp} and $E_{||}$ configuration, for two values of the sphere radius ($R = 15$ and 30 \AA). Such a position for the corresponding isolated single sphere (or for the

chain of noninteracting spheres) is shown for reference. The variation follows an inverse cubic law. The peak position for the typical binary cluster ($R = 15 \text{ \AA}$, $a = 30 \text{ \AA}$) is also shown. The E_{\perp} and $E_{||}$ geometries are indistinguishable. The peak positions are slightly different from those of the independent-sphere plasmon peaks, but cannot be distinguished on the figure.

V. CONCLUSION

Although the presentation of a general theory of absorption by homogeneous spherical microscopic bodies embedded in a matrix are our first aim, we have specialized in our study Sec. III to the case of metallic particles in order to test the numerical tractability of the theory. This has led us in Sec. IV to investigate various parameters of relevance to experimental work. It seems of interest to start our conclusion first with comments pertinent to ex-

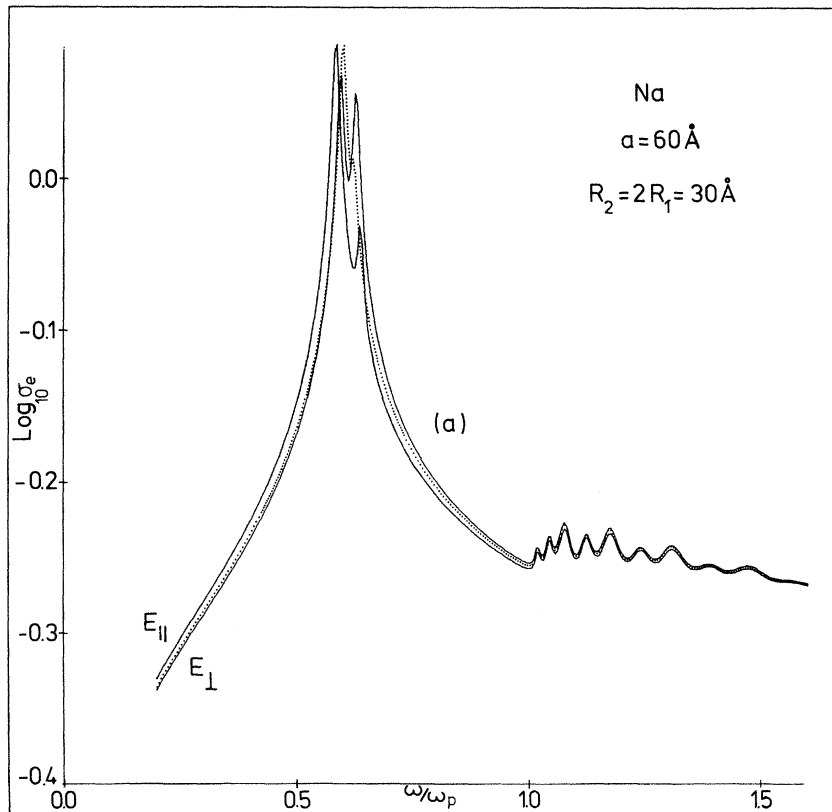


FIG. 7. Logarithm of the extinction cross section σ_e for two separate unequal-sized sodium spheres (with magnetic permeability $\mu = 1$) in a polarized (E_{\perp} or $E_{||}$) plane wave when the sphere separation a varies. The dotted lines correspond to the case of noninteracting spheres: (a) $R_1 = 15 \text{ \AA}$, $R_2 = 30 \text{ \AA}$ ($a = 60$ or 75 \AA); (b) $R_1 = 30 \text{ \AA}$, $R_2 = 60 \text{ \AA}$ ($a = 120$ or 150 \AA); (c) $R_1 = 30 \text{ \AA}$, $R_2 = 60 \text{ \AA}$ ($a = 120 \text{ \AA}$); and (d) $R_1 = 30 \text{ \AA}$, $R_2 = 60 \text{ \AA}$ ($a = 240 \text{ \AA}$).

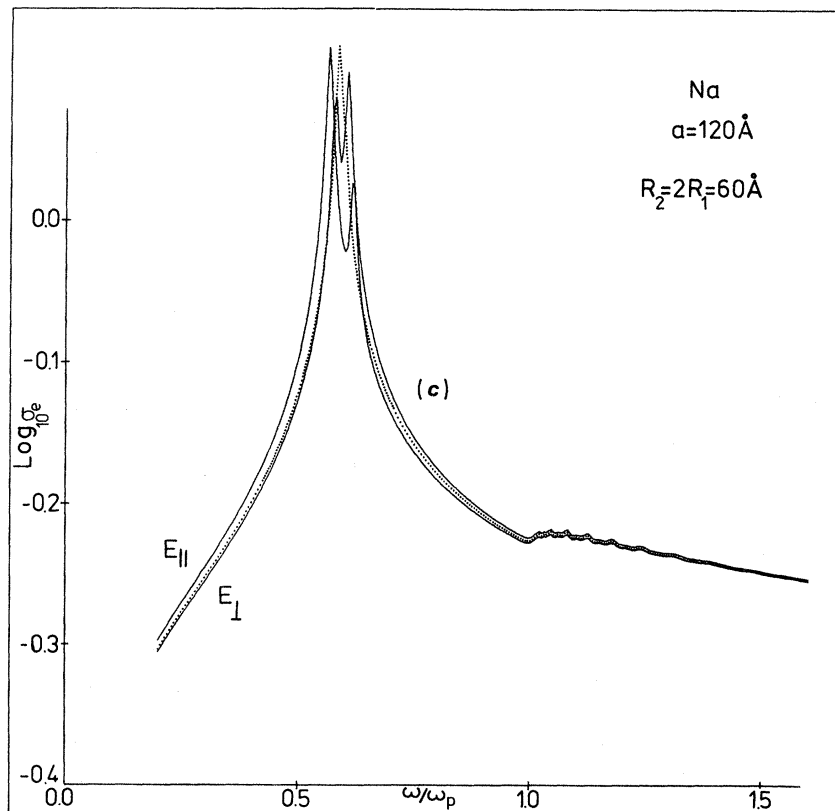
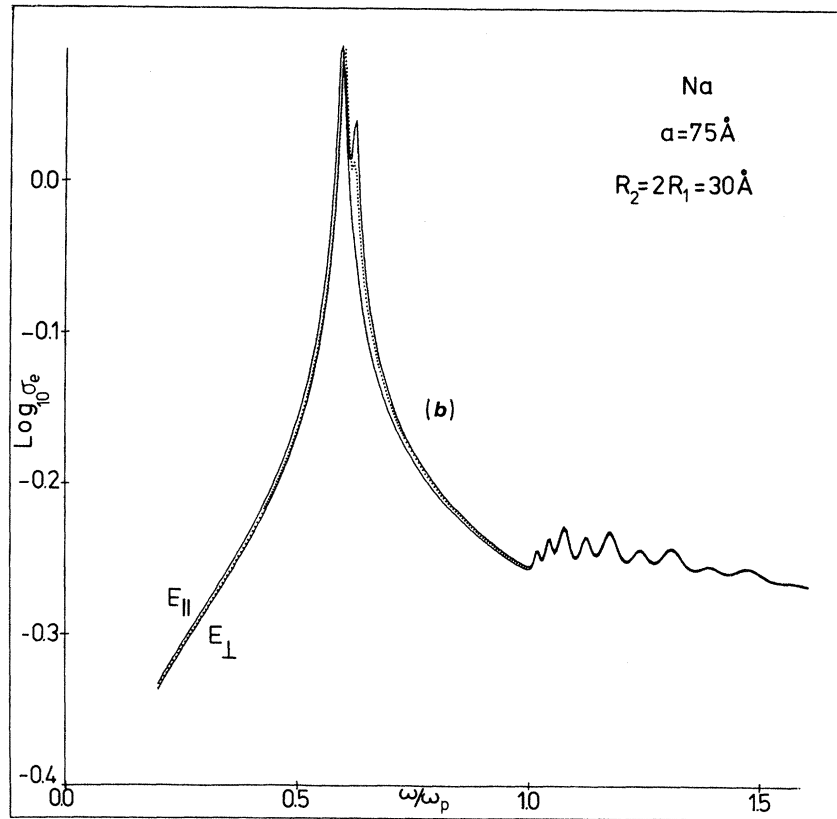


FIG. 7. (Continued.)

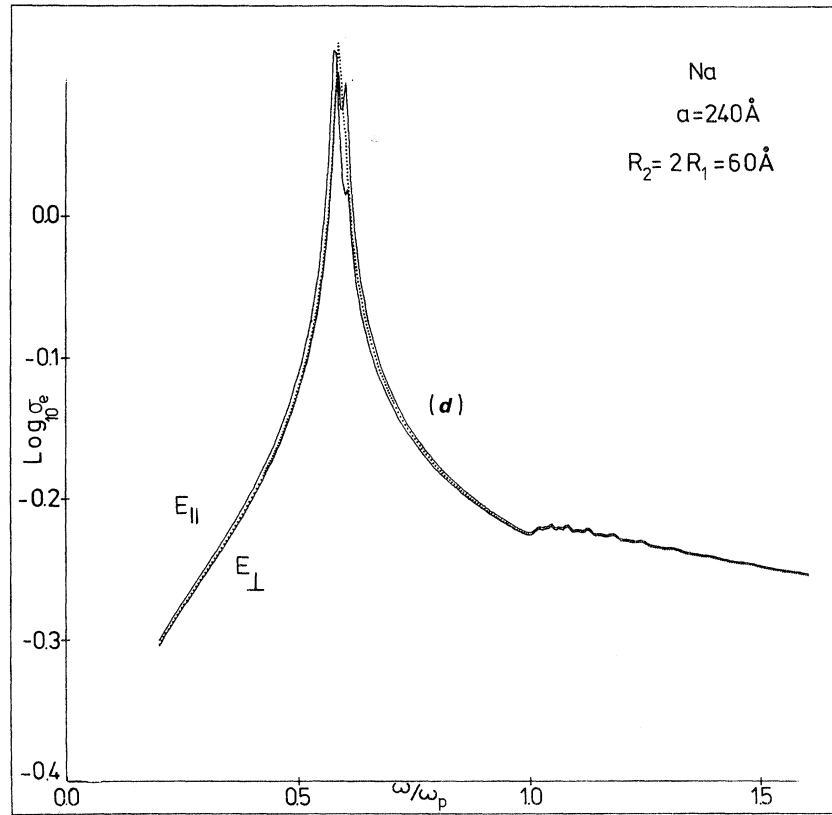


FIG. 7. (Continued.)

perimental observation.

Since no particle is ever isolated, it was of importance to consider the effect of their neighbors. Clearly, effects due to resonant excitation of transverse electromagnetic modes and plasmon modes are dependent on the particle radius as seen experimentally. Several experimental investigations have reported the observation of resonance scattering of light on metallic particles, and in particular on Na.^{31,32} However, the characteristic of the particles is not always clear,³³ and a quantitative comparison to our calculations is not useful. Let us note that we obtain the first plasmon peak at 233 nm, and the main peaks lie between 505 and 310 nm for 15 Å radius particles.

Nevertheless our theoretical investigations allow one to check the importance of clusters in "pure metallic" systems, and to understand deviations from classical theory. It appears, however, that distribution in size of single particles render the observation of fine structure rather difficult. One possibility is to use the angular dependence of the spectrum. Another is to vary the magnetic or electric characteristic of the matrix.

Since the electric dipole-magnetic-dipole coupling factor W_{11}^1 varies like $(ka)^{-2}$, and $ka \simeq 10^{-2}$, while $|\Gamma_1(kR)^3| \simeq 0.06$ as discussed in Sec. IV, it seems unlikely under such normal conditions to obtain a coupling term $W_{11}^1 \Gamma_1 \simeq 10^{-3} (R/a)^3$ large enough to appreciably modify the spectrum through geometrical and dielectric changes. However, when the k -vector magnitude has a larger value, the coupling can be enhanced. This seems feasible if the matrix is chosen such that its permittivity is no more a constant but is frequency dependent, with a value close to the resonance in the appropriate frequency range. On the other hand, the magnetic susceptibility of the spheres Γ_1 can be enhanced if the magnetic permeability of the sphere is close to -2μ , where μ is the matrix magnetic permeability. A *magnetic insulator* (with optical magnon branches) below the magnetic ordering temperature might be considered an interesting matrix. The above theory would be formally unchanged, but Eq. (71) would have to be completed to take into account that k in the matrix has an imaginary part. (An incident plane wave does not exist in such an *infinite* matrix.)

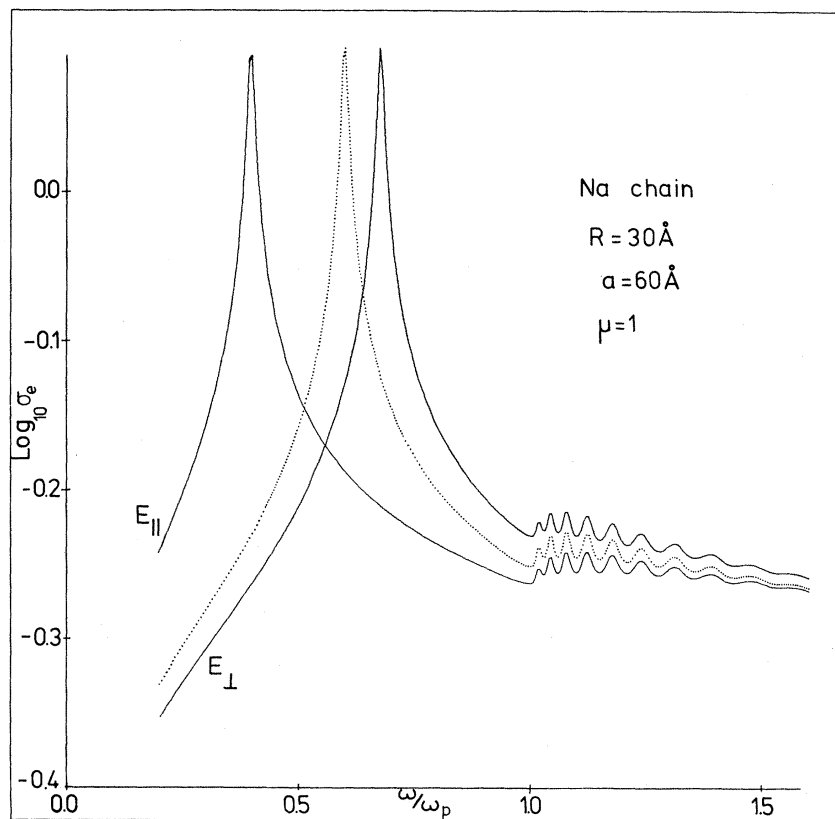


FIG. 8. Logarithm of the extinction cross section σ_e for a linear chain of regularly ordered and spaced sets of equal-sized sodium spheres ($\mu=1$) in vacuum, $R_i=R=30 \text{ \AA}$, $a=60 \text{ \AA}$ for different field polarization.

From a purely theoretical point of view, our theory seems to be the most general one with respect to experimental work, except for the hypothesis of spherical shape of the particles and the neglect of quantum and thermodynamic effects. The inclusion of multipolar interaction to all orders has been simple. No calculation on their effect has been made, but it would be interesting to observe whether, e.g., quadrupolar effects become relevant when interpreting spectra, in particular for aggregated systems. Retardation effects have been also included. Furthermore the formalism achieves some interesting simplification since it separates the microscopic physics (calculation of susceptibilities) from the submicroscopic ones (calculation of interactions); hence, the position of the resonances and the "structure" of plasma peaks are clearly understood as arising from different mechanisms [Eq. (92)]. Further theoretical extensions would include inhomogeneity effects and statistical effects (based on knowledge of the size distribution and information such as the pair correlation function). Other experimental geometries (spherical incident wave, etc.) are immediately described from equations of

Sec. III.

The simplifications of Langbein's differential recurrence relation into a pure recurrence relation is not a small step. Compare, for example, tables of Appendix B with those of Ref. 24, and see that ours allow the inclusion of high-multipole interaction effects in any calculation.

Clanget was the first to predict the appearance of secondary structure above ω_p for isolated spheres.¹⁴ Ruppin's inclusion of k -dependent damping found no shift in the position of such a secondary structure. We have shown here that interaction effects are quasi-irrelevant for this position, and have only some effects on the magnitude of the absorption of the plasmon peaks. However, Clanget did not discuss the main resonant peak, while Ruppin's results obviously apply in the weak density limit. We have shown the important influence of proximity effects, and necessarily of light polarization and angle of incidence effects, as in the case of ionic crystals.

We have pointed out the danger of using a simple form for the damping factor. Even though such a damping is introduced to compensate for an

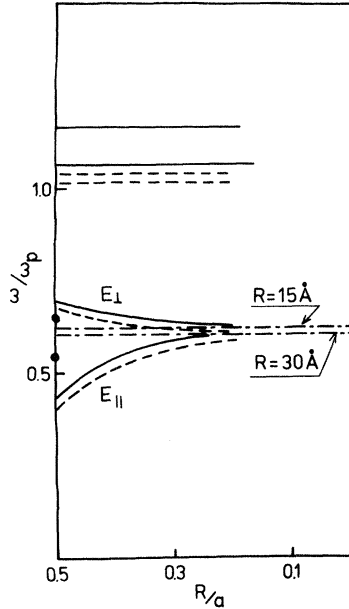


FIG. 9. Variation of characteristic peak positions for the extinction cross section of a linear chain of regularly ordered and spaced sets of two equal-sized ($R_i = R$) sodium spheres ($\mu = 1$) in vacuum as a function of the separation ratio (R/a). The size effect is shown by full or dashed lines, corresponding to radii $R = 15$ or 30 Å, respectively. The field-polarization geometry is indicated. The lower curves correspond to the main "dipolar" resonance; the upper curves show the position and variation of the first two plasmon peaks. The dot-dash line is the Frohlich resonance mode for noninteracting spheres (Ref. 15). The positions of the main resonances for the simplest binary-cluster case ($R_1 = R_2 = 15$ Å) are indicated by heavy dots.

unrealistic dielectric function, (it might be refined at a later stage), it would be useful to choose a more sophisticated dielectric function. The same holds true for the magnetic permeability. Another point on the damping factor is in order: the same damping was used for ϵ^T and ϵ^L . Different damping factors might be a more realistic situation, but we expect no drastic qualitative difference on the observations made here: the shift of the main resonance due to interaction between particles and the modification of the high-frequency structure.

After this work was completed, we came across some older work on optical properties of aggregated metal systems, based on Maxwell-Garnett theory, within the low-damping regime ($\omega_p \tau > 1$), and on a numerical calculation in the moderate and high-damping regime ($\omega_p \tau \leq 1$), taking into account some dielectric matrix effect.³⁴ Shifts of the main absorption peaks were discussed in the

quasistatic limit ($k = 0$), but no expression was derived for the "respective resonance frequencies due to complicated algebra" (*sic*) in the presence of plasmons.

ACKNOWLEDGMENT

One of us (J.M.G.) would like to thank the "Institut pour la Recherche Scientifique dans l'Industrie et l'Agriculture" (IRSIA), Brussels, Belgium, for financial support.

APPENDIX A

Relations between the Legendre functions $P_n^m(x)$ necessary in the calculation of the transposition of frames are given without detailed proof. In the calculation of Eq. (24), after separating the terms in $z_{q-1}(r)$ and $z_{q+1}(r)$, two expressions contain Legendre functions:

$$I_1 = n \sin \theta P_n^m(\cos \theta) - \frac{dP_n^m(\cos \theta)}{d \cos \theta} \cos \theta \sin \theta - m \frac{P_n^m(\cos \theta)}{\sin \theta} \quad (\text{A1})$$

$$I_2 = (n+1) \sin \theta P_n^m(\cos \theta) + \frac{dP_n^m(\cos \theta)}{d \cos \theta} \cos \theta \sin \theta + m \frac{P_n^m(\cos \theta)}{\sin \theta} \quad (\text{A2})$$

In Ref. 29, Eq. (8.733.1) reads (with $u = \cos \theta$)

$$(1-u^2) \frac{dP_n^m(u)}{du} = -n u P_n^m(u) + (n+m) P_{n-1}^m(u) \quad (\text{A3})$$

$$= (n+1) u P_n^m(u) - (n-m+1) P_{n+1}^m(u) \quad (\text{A4})$$

Using those identities, one can rewrite I_1 and I_2 , i.e.,

$$I_1 = (1-u^2)^{-1/2} [(n-m) P_n^m(u) - (n+m) u P_{n-1}^m(u)], \quad (\text{A5})$$

$$I_2 = (1-u^2)^{-1/2} [(n+m+1) P_n^m(u) - (n-m+1) u P_{n+1}^m(u)], \quad (\text{A6})$$

which with Eqs. (8.735.1) and (8.735.2) from Ref. 29 immediately lead to

$$I_1 = P_{n-1}^{m+1}(u) \tag{A7}$$

$$I_2 = -P_{n+1}^{m+1}(u) . \tag{A8}$$

In calculating Eq. (27),

$$I_3 = n \cos\theta P_n^m(\cos\theta) + \sin^2\theta \frac{dP_n^m(\cos\theta)}{d \cos\theta} \tag{A9}$$

$$I_4 = -(n+1)\cos\theta P_n^m(\cos\theta) + \sin^2\theta \frac{dP_n^m(\cos\theta)}{d \cos\theta} \tag{A10}$$

appear, and are transformed by substituting Eq.

(8.733.1) of Ref. 29 into

$$I_3 = (n+m)P_{n-1}^m(\cos\theta) \tag{A11}$$

$$I_4 = -(n-m+1)P_{n+1}^m(\cos\theta) . \tag{A12}$$

APPENDIX B

In numerical work, functions $V_{nq}^m(a)$ and $W_{nq}^m(a)$ as defined by Eq. (43) are calculated in terms of the solution of the recurrence relation (40) for $\mathcal{L}_{n,q}^m(a)$. In order to facilitate an analytical calculation of these terms, concise and explicit expressions of the $V_{nq}^m(a)$'s and the $W_{nq}^m(a)$'s can be obtained as expansions, clearly showing the asymptotic values of the interaction terms to be used in

TABLE I. Spherical coupling parameters as defined in the text for the functions $V_{n,q}^m(a)$ defined in Appendix B [Eqs. (B1) and (43a)]. The set in rectangles corresponds to the parameters v_k calculated by Langbein (Ref. 24). The difference in value arises from different normalizations.

<i>m</i>	<i>n</i>	<i>q'</i>	0	1	2	3	4	5	6	7	8	9	
0	1	1	0	0	2	2							
		2	0	0	2	6	6						
		3	0	0	2	12	30						
		4	0	0	2	20	90		30				
	2	2	0	0	2	10	24		210				
		3	0	0	2	16	66		150	150			
		4	0	0	2	24	150		570	1260	1260		
		3	0	0	2	22	135		510	1125	1125		
		4	0	0	2	30	255		1410	5085	11 025	11 025	
		4	0	0	2	38	423		3174	16 485	57 645	123 480	123 480
1	1	1	2	2	2								
		2	2	6	12	12							
		3	2	12	42	90	90						
		4	2	20	110	390	840	840					
	2	2	2	10	42	96	96						
		3	2	16	102	402	900	900					
		4	2	24	210	1230	4590	10 080	10 080				
		3	2	22	207	1230	4606	10 125	10 125				
		4	2	30	375	3090	16 965	16 065	132 300	132 300			
		4	2	38	623	6774	50 685	263 445	922 005	1 975 680	1 975 680		
2	2	2	4	12	24	24							
		3	10	60	210	450	450						
	3	3	18	180	990	3510	7560	7560					
		3	25	225	1275	4650	10 125	10 125					
		4	45	585	4725	25 650	91 800	198 450	198 450				
		4	81	1377	15 039	113 130	590 625	2 072 385	4 445 280	4 445 280			
		3	3	25	150	525	1125	1125					
			4	105	1050	5775	20 475	44 100	44 100				
4	441	6174	49 245	260 925	919 485	1 975 680	1 975 680						
4	4	294	2940	16 170	57 330	123 480	123 480						

TABLE II. Spherical coupling parameters entering the definition of function $W_{n,q}^m(a)$ [Eqs. (B2) and (43b)]. The set in rectangles corresponds to the parameters w_k calculated by Langbein (Ref. 24). The numerical difference for these arises from different normalizations.

m	n	q	0	1	2	3	4	5	6	7		
1	1	1	2	2								
		2	2	6	6							
		3	2	12	30	30						
		4	2	20	90	210	210					
	2	2	2	2	10	24	24					
		3	2	2	16	66	150	150				
		4	2	2	24	150	570	1260	1260			
		3	3	2	22	135	510	1125	1125			
	3	4	4	2	30	255	1410	5085	11 025	11 025		
		4	4	2	38	423	3174	16 485	57 645	123 480	123 480	
		2	2	4	12	12						
			3	10	60	150	150					
3	3	3	25	225	975	2250	2250					
	4	4	45	585	3825	14 850	33 075	33 075				
	4	4	81	1377	12 339	69 930	255 150	555 660	555 660			
	3	3	3	25	150	375	375					
4	4	4	105	1050	4725	11 025	11 025					
	4	4	441	6174	41 895	165 375	370 440	370 440				
4	4	4	294	2940	13 230	30 870	30 870					

considering effects of small or large wave numbers or of various distances between particles. For $m \geq 0$, we can write

$$V_{n,q}^m(a) = N_{nq}^m \frac{e^{ia}}{a^m} \sum_{j=0}^{q+n-m+1} i^j v_{n,q}^m(j) a^{-j} \quad (B1)$$

$$W_{n,q}^m(a) = -N_{nq}^m \frac{e^{ia}}{a^m} \sum_{j=0}^{q+n-m} i^j w_{n,q}^m(j) a^{-j} \quad (B2)$$

with

$$N_{nq}^m = i^{n-q-m} (m!)^2 n(n+1)q(q+1)A_{nq}^m / 4, \quad (B3)$$

where the A_{nq}^m 's are defined by Eq. (44). The coefficients $v_{nq}^m(j)$ and $w_{nq}^m(j)$ are given for $1 \leq n, q \leq 4$ and $0 \leq m \leq 4$ in Tables I and II. This allows one

to treat interactions up to the $(2^4, 2^4)$ polar order. The factor N_{nq}^m has been so chosen such that v_{nq}^m and w_{nq}^m become integers. Notice that

$$v_{nq}^m(j) = v_{qn}^m(j) \quad (B4)$$

$$w_{nq}^m(j) = w_{qn}^m(j) \quad (B5)$$

imply the additional relations

$$\begin{Bmatrix} V_{nq}^m(a) \\ W_{nq}^m(a) \end{Bmatrix} = (-1)^{n+q} \begin{Bmatrix} V_{qn}^m(a) \\ W_{qn}^m(a) \end{Bmatrix}. \quad (B6)$$

The use of the second table must be completed by the relation

$$w_{nq}^0(j) = 0. \quad (B7)$$

The elements which are not written in the tables are identically zero.

¹J. M. Gérardy and M. Ausloos, Phys. Rev. B **22**, 4950 (1980).

²J. M. Gérardy and M. Ausloos, Surf. Sci. **106**, 319 (1981).

³M. Ausloos, P. Clippe, and J. M. Gérardy, Le Vide,

Les Couches Minces, Suppl. **21**, 758 (1980).

⁴J. M. Gérardy and M. Ausloos (unpublished).

⁵O. F. Hagena, Surf. Sci. **106**, 101 (1981).

⁶W. D. Knight, Surf. Sci. **106**, 172 (1981).

- ⁷C. G. Granqvist, N. Calander, and O. Hunderi, *Solid State Commun.* **31**, 249 (1979), and references therein.
- ⁸E. Simanek, *Phys. Rev. Lett.* **38**, 1161 (1977); *Solid State Commun.* **31**, 419 (1979).
- ⁹W. Lamb, D. M. Wood, and N. W. Ashcroft, in *Electrical Transport and Optical Properties of Inhomogeneous Media (Ohio State University, 1977)*, Proceedings of the First Conference on the Electrical Transport and Optical Properties of Inhomogeneous Media, edited by J. C. Garland and D. B. Tanner (American Institute of Physics, New York, 1978), p. 240.
- ¹⁰P. Clippe, R. Evrard, and A. A. Lucas, *Phys. Rev. B* **14**, 1715 (1976).
- ¹¹M. Ausloos, P. Clippe, and A. A. Lucas, *Phys. Rev. B* **18**, 7176 (1978).
- ¹²G. Mie, *Ann. Phys. (Leipzig)* **25**, 377 (1908).
- ¹³P. J. Wyatt, *Phys. Rev.* **127**, 1837 (1962).
- ¹⁴R. Clanget, *Optik (Stuttgart)* **35**, 180 (1972).
- ¹⁵R. Ruppin, *Phys. Rev. B* **11**, 2871 (1975).
- ¹⁶J. Stratton, *Electromagnetic Theory* (McGraw-Hill, New York, 1941).
- ¹⁷P. M. Morse and H. Feshbach, *Methods of Theoretical Physics* (McGraw-Hill, New York, 1953).
- ¹⁸M. Abramowitz and I. A. Stegun, *Handbook of Mathematical Functions* (Dover, New York, 1972).
- ¹⁹A. R. Melnyk and W. Harrison, *Phys. Rev. B* **2**, 835 (1970).
- ²⁰L. Néel, e.g., in *Low Temperature Physics*, edited by C. Dewitt, B. Dreyfus, and P. G. DeGennes (Gordon and Breach, New York, 1962), p. 413.
- ²¹M. Figlarz, F. Vincent, C. Lecaille, and J. Amiel, *Powder Technol.* **1**, 121 (1967).
- ²²P. Mollard, A. Collomb, J. Devenyi, A. Rousset, and J. Paris, *IEEE Trans. Magn.* **MAG-11**, 894 (1975).
- ²³W. Hayes and R. London, *Scattering of Light by Crystals* (Wiley, New York, 1978), e.g., p. 256.
- ²⁴D. Langbein, *Springer Tracts in Modern Physics*, Vol. 72 (Springer, Berlin, 1974).
- ²⁵B. Jeffreys, *Geophys. J. R. Astron. Soc.* **10**, 141 (1965).
- ²⁶Notice the difficulty inherent in this form of ρ (Ref. 15). When no longitudinal polarization wave can propagate in the spheres, the imaginary part of k^L becomes infinitely large. This physical case corresponds to the classical Mie theory. However, if $k^L = k_1^L + ik_2^L$, ρ given by Eq. (78) becomes
- $$\rho = \rho_0 + \eta(k_1^{L2} + k_2^{L2} + 2ik_1^L k_2^L) / k_F^2.$$
- If $k_2^L \rightarrow \infty$, $\text{Re}\rho \rightarrow -\eta(k_2^L/k_F)^2$ becomes infinitely large and negative. This unrealistic situation can be alleviated if another expression is assumed for ρ , i.e., with $\tilde{\eta} = (\eta/\rho_0)^{1/2}$,
- $$\rho = \rho_0 \cosh(\tilde{\eta} k^L / k_F)$$
- which reduces to Eq. (78) in the case $|k_1^L/k_F| \ll 1$ and is finite for large values (in the plasmonless case).
- ²⁷M. S. Haque and K. L. Kliever, *Phys. Rev. B* **7**, 2416 (1973).
- ²⁸C. Kittel, *Introduction to Solid State Physics* (Wiley, New York, 1968), p. 448.
- ²⁹I. S. Gradshteyn and I. M. Ryzhik, *Table of Integrals, Series and Products* (Academic, New York, 1965).
- ³⁰M. Ausloos and J. M. Gérardy (unpublished).
- ³¹C. J. Duthler, S. E. Johnson, and H. P. Broida, *Phys. Rev. Lett.* **26**, 1236 (1971).
- ³²D. M. Mann and H. P. Broida, *J. Appl. Phys.* **44**, 4950 (1973).
- ³³J. Hecht, W. P. West, and H. P. Broida, *J. Chem. Phys.* **71**, 3132 (1979).
- ³⁴J. P. Marton and J. R. Lemon, *J. Appl. Phys.* **44**, 3953 (1973).